AERITALIA
società aerospaziale italiana
IRI finmeccanica
Space Systems Group

TETHERED GRAVITY LABORATORIES STUDY

CONTRACT NAS 9-17877

QUARTERLY PROGRESS REPORT # 6

FOR THE PERIOD

25 MAY 1989 THROUGH 24 AUGUST 1989

SEPTEMBER 1989

(NASA-CR-185658) TETHERED GRAVITY LABORATORIES STUDY Quarterly Progress Report No. 6, 25 May - 24 Aug. 1989 (Aeritalia S.p.A.) 88 p
CSCL 22A
N91-30349
Unclas
G3/29 0036883

Prepared for :

NATIONAL AERONAUTICS AND SPACE ADMINISTRATION

LYNDON B. JOHNSON SPACE CENTER

HOUSTON TX-77058

PROGRESS REPORT

TITLE : QUARTERLY PROGRESS REPORT # 6

D.R.D. No :

---------- SIGNATURES AND APPROVALS ON ORIGINAL ----------

PREPARED : STUDY TEAM
CHECKED : L. CONDELLO
APPROVED : L. AMELOTTI
AUTHORIZED : L.M. QUAGLINO

APPROVALS : on

STUDY MANAGER P. MERLINA

22 SET '89

DATA MANAGEMENT : 25/09/89

DOCUMENT CHANGE RECORD

ISSUE-DATE	REASONS FOR CHANGE	AFFECTED PARAGRAPHS
01 25/AUG/89		

All information contained in this document are property of AERITALIA S.A.I.p.A.. All rights reserved.
AERITALIA S.A.I.p.A. CAP. LIT. 337.500.000.000 INT. VERS.
TRIBUNALE NAPOLI N. 777/69 C.C.I.A. NAPOLI N. 269965.

TABLE OF CONTENTS

1.0 INTRODUCTION

This is the 6th quarterly progress report submitted by AERITALIA - GSS (AIT) under contract NAS9-17877 "Tethered Gravity Laboratories Study". This report covers the period from 25 MAY 1989 through 24 AUGUST 1989.

2.0 TECHNICAL STATUS

2.1 WORK ACCOMPLISHED DURING REPORTING PERIOD

During the reporting period, the task 3.0 (Variable Gravity Laboratory) was carried on according to the Study Schedule.

2.1.1 Variable Gravity Laboratory

2.1.1.1 Conceptual Design & Engineering Analysis (AIT)

a) VGL thermal control issues were analysed to outline the configuration problems and their possible solutions.
Basic topics of VGL thermal control system are the payload heat loads variability (depending on the particular mission) and the microgravity requirements that limit the acceptable amount of mechanical noise.

b) The attitude control problem was analysed with particular reference to the tether - VGL interaction in terms of forces and torques.

c) Attitude control system sensors and actuators were tentatively defined.
ACS concept will be refined on the basis of the SAO attitude dynamics simulations.

d) Overall VGL configuration constraints were evaluated in terms of G-level, access, payload replacement, surface constraints and slot configuration.

e) The payload configuration was analysed at a conceptual level. A removable payload module configuration was selected in order to allow high flexibility in the payload accommodation.

f) See Appendix A for technical discussion of the above points.

g) The conceptual design and engineering analysis of VGL was basically completed during reporting period.
The overall VGL configuration problem will be further investigated under the "Technology Requirements" subtask.

2.1.1.2 Control Strategies (SAO)

a) The analysis of the accelerations acting on board VGL has been continued.
Specifically the activity was focused on the attitude dynamics of the VGL.

b) Numerical simulations have been run to show the effects of attitude motion on the acceleration field on board VGL, namely:
1. Station keeping at 2667 m off the Space Station
2. VGL crawling from 2667 m to 10242 m
3. Same as 2 but with the in-plane libration/lateral dampers activated.

c) See Appendix B for detailed technical discussion.

2.1.1.3 Technology Requirements (AIT)

a) The VGL accelerometers requirements were updated.

b) Accelerometers currently available for space applications were reviewed and discussed.

c) Accelerometers under study or development were analysed in order to assess the foreseen performances.

d) Compliance of existing or under development accelerometers with VGL requirements was assessed and preliminary technology requirements were discussed.

e) See Appendix A for detailed technical discussion.

2.2 WORK PLANNED FOR THE NEXT REPORTING PERIOD

2.2.1 Variable Gravity Laboratory

a) Technology Requirements (AIT)
The conceptual configuration of the VGL system will be investigated in terms of payload module technology, VGL technology and VGL system interfaces with the Space Station.

b) Control Strategies (SAO)
The analysis of VGL attitude dynamics will be continued to provide information for the definition of the attitude control system.

2.2.2 Attitude tether stabilizer

Activities relevant to this task will be started during next reporting period as soon as Statement of Work modifi-

3.0 SCHEDULE ASSESSMENT

During this reporting period the planned activities shown on the attached schedule have been performed as follows:

ACTIVE C.o.G. CONTROL

- All activities relevant this task are completed.

Low Gravity Processes Identification

- Completed 100%

Variable Gravity Laboratory

- Concept Design & Engineering Analysis has been completed during reporting period.
- Technology Requirements is in progress 50% completed.
- Control strategies is in progress 70% completed.

The activities control strategies and technology requirements relevant to the Active C.o.G. Control task have not been started, as agreed between Aeritalia and NASA-JSC.

AERITALIA
SPACE SYSTEMS GROUP

DEPARTMENT:

PROGRAM : TETHERED GRAVITY LABORATORY STUDY

TASK/W.P./C.I. : MASTER BAR CHART

REMARKS:
▽ = H.Q.
⊽ = JSC

PREPARED	L. CONDELLO	DOCUMENT N°TG-CH-A1-001
CHECKED	G. REINAUD	ISSUE 1
APROVED	L. AMELOTTI	PAGE 1 OF 1
PROJ. CONTR	L. CONDELLO	DATE 01.03.88
PROGRAM MANAGER	P. MERLINA	STATUS DATE 22/02/89

N°	DESCRIPTION
1	
2	MANAGEMENT & PROJECT CONTROL
3	PROGRESS REPORT
4	MEETINGS & REVIEWS
5	
6	"ACTIVE C.O.G. CONTROL"
7	FORCE-FIELD CHARACTERIZATION
8	MATHEMATICAL MODELS REVIEW
9	CONFIGURATION ANALYSIS
10	CONTROL STRATEGIES
11	TECHNOLOGY REQUIREMENTS
12	
13	"LOW GRAVITY PROCES. IDENTIF."
14	
15	"VARIABLE GRAVITY LABORATORY"
16	CONCEPT DESIGN & ENGINEERING ANALYSIS
17	CONTROL STRATEGIES
18	TECHNOLOGY REQUIREMENTS
19	
20	
21	
22	

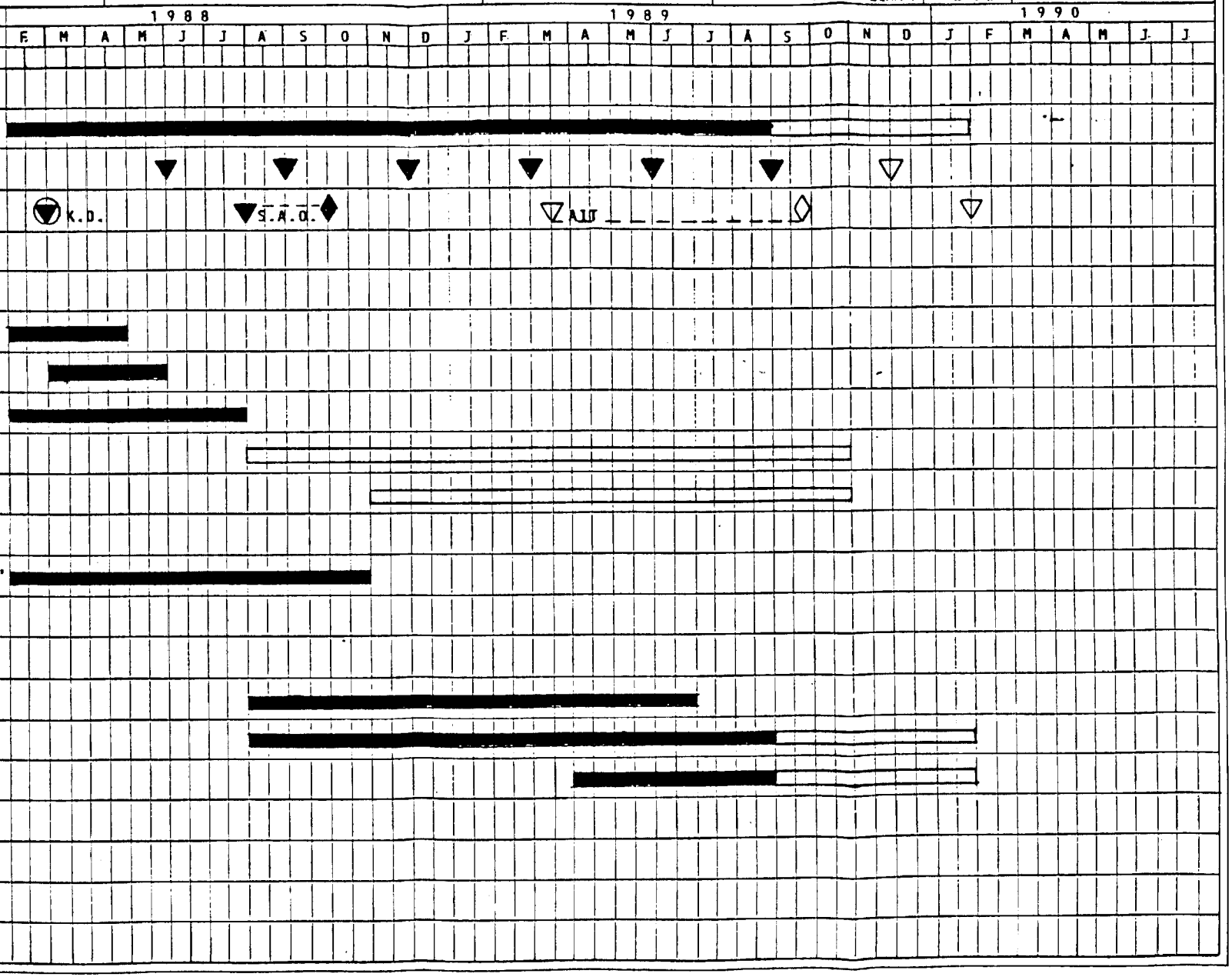

4.0 PROBLEMS AND CONCERNS

No problems encountered during reporting period.

APPENDIX A

VARIABLE GRAVITY LABORATORY

1. THERMAL CONTROL ISSUES

1.1 GENERAL

A meaningful thermal control definition typically requires a degree of detail and a "frozen" configuration which are available only in late stage of system design. What can be done at this very first level of analysis is more the underlining of the foreseeable problems and a review of their possible solutions with their advantages and drawbacks.

The points which drives the VGL thermal control subsystem are, in brief:
1) Low earth orbit, with low inclination which implies a short duration thermal cycle, with the VGL which can be alternatively in full Sun or completely in shadow.
2) The heat loads from and to the payload is not known now, and in general will change depending on the mission. It is evident that many variable g experiments involving material phase change will require a tight thermal control with large thermal power.
3) The microgravity condition which should be attained limits the amount of mechanical noise which can be accepted (active fluid loop system requiring a pump is a drawback)
4) The variable g environment can have an impact on the performance of certain pieces of hardware. Here we are thinking to the heat pipes which, under the artificial gravity achieved on the VGL, can change their ability to transfer heat (convection can either help or hinder heat transfer).

1.2 ASSUMPTIONS

An initial set of assumptions has to be made just to start the discussion of the thermal control subsystem.

First of all a general idea of the shape and size of the VGL is required.
For a start a 1.5 m high and 1.5 m diameter cylinder can be used (this will be justified in the following configuration analysis). The longitudinal axis of the cylinder is parallel to the tether direction. (See fig. 1.1)

The assumed maximum heat load due to the payload and services is 400 W plus 100 W due to electrical losses in the batteries (80 % efficiency).
The minimum heat leak from the payload and services is 0 with still 100 W from the batteries. The idea in this case is that all the electrical power is used to heat experiments involving material phase change. If less power were

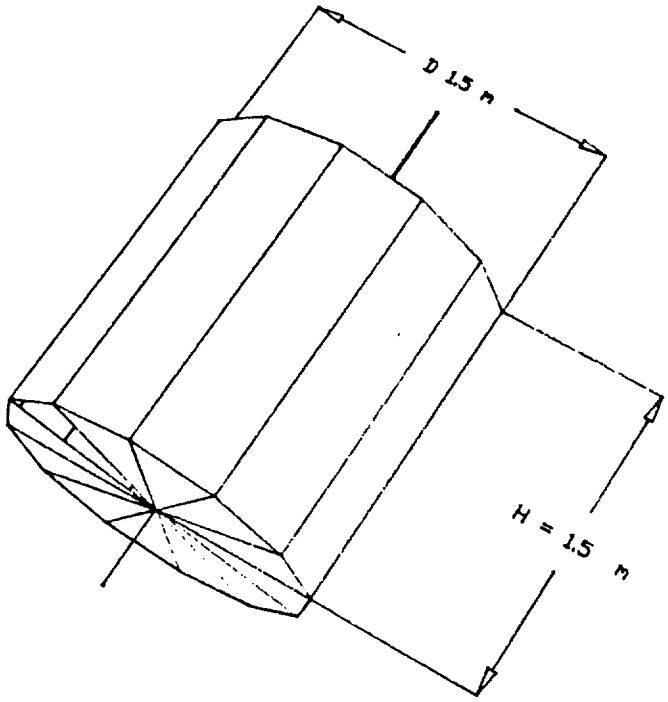

Fig. 1.1 VGL configuration (calculation purpose only)

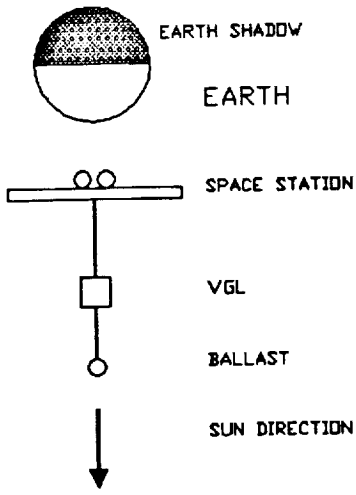

Fig. 1.2 - "Hot" case VGL position

required from the payload and equipments more would be available to the thermal control.

A 200 W maximum power allocation to the thermal subsystem is assumed.

The range of acceptable temperature goes from 258 K to 313 K. This is to be understood as an average global value more useful as a reference than for calculation. In fact some components (notably batteries) have in general a more stringent requirement.

1.3 "ZERO ORDER" ANALYSIS

The simplest possible thermal model of the VGL can be made assuming that all the VGL surfaces have the same value of emittance and absorptance.

For the hottest condition the Sun is assumed to be straight along the tether direction at the orbit noon (actually the worst case depends on the effective values of absorptance and emittance). See fig. 1.2.
The coldest condition takes place when the VGL is in the Earth shadow.

Under these further assumptions we are able to calculate the effective areas and the impinging radiation (which is different from the actual radiative loads due to the thermo-optical surface properties) involved in the thermal exchange (see table 1.1).
Given that only the Earth generated heat is present when the VGL is in shadow there is a ratio of almost 6 to 1 in the impinging radiation from full Sun view to Earth shadow.

The equation governing the thermal problem are

$$\text{Input power} = J_s\ \alpha\ (As + a\ Aa) + J_t\ \varepsilon\ A_e + P + Pb + Pt$$
$$\text{Output power} = \delta\ \varepsilon\ T^4\ A_t$$

J_s = Sun heat flux = 1327 W/m^2

J_t = Earth heat flux = 237 W/m^2

a = Earth albedo = 0.37

Aa = effective area for albedo = 3.72 m^2

As = effective area for Sun flux = 1.77 m^2

Ae = effective area for Earth flux = 3.66 m^2

At = overall geometrical area = 10.6 m^2

	Space Station base	lateral surface	ballast looking surface	Total
Geometrical Area (m^2)	1.770	7.050	1.770	10.590
Sun view factor	0.000	0.000	1.000	
Sun effective areas (m^2)	0.000	0.000	1.770	1.770
Earth view factor	0.893	0.296	0.000	
Earth effective area (m^2)	1.581	2.085	0.000	3.665
Earth albedo view factor	0.900	0.303	0.000	1.203
Albedo effective area (m^2)	1.593	2.133	0.000	3.726

Table 1.1 - VGL thermal calculation parameters

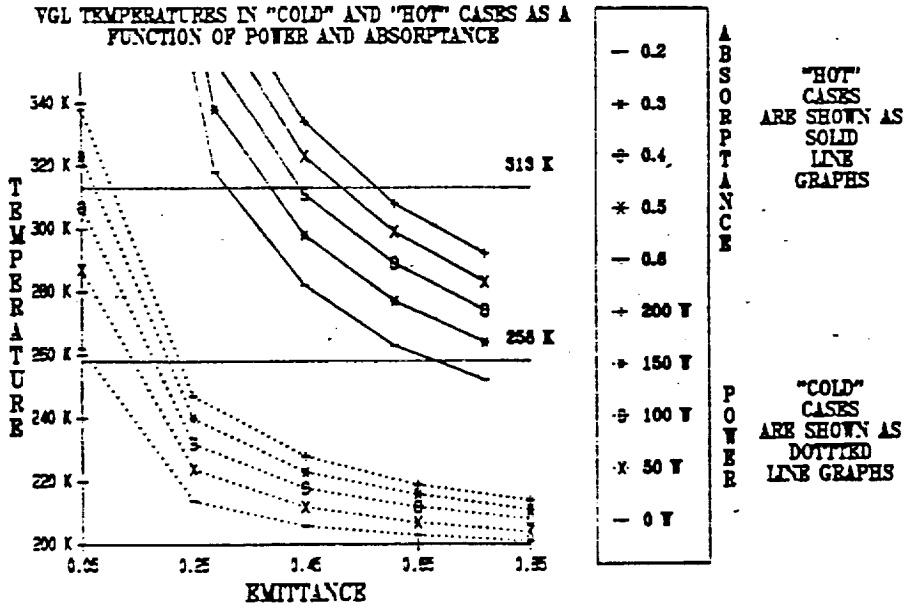

Fig. 1.3 - VGL temperature in 'hot' and 'cold' cases

P = power input from equipments and payloads (0 in shadow, 400 W in Sun view)

Pb = power loss in batteries = 100 W

Pt = power available for thermal control = up to 200 W

T = equilibrium temperature (Kelvin)

For computing the "hot" case temperature a wide range of absorptance values and emittance values was swept (the fact that emittance and absorptance are not independent was neglected).

For computing the "cold" case temperature the same range of emittance values and a 0 to 200 W range of heaters power were swept (absorptance is not a factor in this case).

The resulting temperature for "hot" and cold cases are reported in fig. 1.3 respectively as solid and dotted line graphs.

It can be seen that no parameter combination can satisfy both the requirement for the highest and lowest temperature. Moreover from the graphs it can be deduced that the "hot" case is rather easy to deal with, whereas only with very low emittance the lowest temperature can be kept over the 258 K limit. This is not to say that passive thermal control is inadequate in any case, but merely that it is not the "natural" behaviour of the VGL.
As a last point it should be noted that given the relatively short duration of the orbit the thermal capacity of the system should be taken in account thus limiting extreme temperatures.

1.4 THERMAL CONTROL OPTIONS

There are at least three kinds of thermal control options:

1) Purely passive system.
With a careful combination of emittance, absorptance of external surfaces, conductance and heaters location it should be possible to meet the temperature requirements with a reasonable amount of power. After all, most satellites are controlled in temperature just in this way.
On the other hand the variability of payloads, which is intrinsic to the VGL, implies that one basis for passive thermal control, a good knowledge of internal heat loads, is lacking. In other words a passive thermal design is

general rule, a thorough redesign (and reconfiguration) of the VGL thermal control subsystem.

2) Semi active system
In this set we include all the systems involving components which are able to change the radiative properties of external surfaces and which can change their conductance (as variable capacity heat pipes).
The advantage of these systems is that they offer a capability to deal with drastic change in the heat loads (which would be due to payload changes) which is greater than that of the purely passive systems.
The main drawback is the resulting increased complexity of the system and hence the reduced reliability. For a system like the VGL which can be checked out in space just prior to the mission start and that can be recovered in a matter of hours this point is somewhat less decisive than for other space systems.

3) Active system
Here we mean those systems which include a cooling fluid loop activated by a pump. In general they offer the largest degree of flexibility which has to be traded off again with the complexity and, more to our point, with an unavoidable amount of mechanical noise. In the VGL microgravity application this is a serious drawback even though low noise pumps are being developed just for this purpose.
Another point worth mentioning is the fact that interfacing the fluid loop with the payload can be not a trivial task .

A component which can be useful to all these systems is a tank containing material which can undergo phase change within the required temperature envelope. This can act as a damper in the thermal cycle and given the relative short orbital period should not require a large amount of mass.

At a first, conceptual level of trade off it appears that semi passive system (eventually used in conjunction with phase change material) are the best choice. If the amount of heat to be disposed off is too large then an active system, with careful location of the active mechanical components is our second choice. A purely passive system does not appear consistent with the expected required performances.

1.5 ANALYSIS SUMMARY

1) The VGL has a significant thermal control problem due to the extreme variation on radiative environment and to the large variability on the payload which is assumed.

2) In a first evaluation, semi passive systems (with louvers, shutters and variable capacity heat pipes) appear the best choice followed by active fluid loop system. Phase change material with their ability to store large amount of heat can be helpful in reducing extreme temperatures.

This first glance at the thermal control problems will be integrated with further detail when treating the overall VGL configuration.

2. ATTITUDE CONTROL SUBSYSTEM

2.1 GENERAL

The VGL presents a special case of attitude control problems. In fact:
1) First of all it is not a "free flyer" but it is able to exchange forces and torques with the tether. Around the pitch and roll axis these interactions dominate all other effects.
2) On top of a rather coarse requirement on the pointing, we have a stringent requirement on the angular speeds and accelerations which can be translated as disturbance to the VGL gravity level.

So a first analysis of the ACS is deemed necessary even at this very preliminary stage to clarify the main issues involved.

The reference frame used in the discussion is centred on the VGL center of mass and with the same orientation of axes as the Space Station reference frame. That is

X axis = flight direction = roll axis
Y axis = out of orbital plane = pitch axis
Z axis = local vertical = yaw axis

See also fig. 2.1

2.1 ACS REQUIREMENTS

As already said the requirement on the pointing can be rather coarse being driven mainly by the demands of some equipments as solar arrays (if present), radiators, and communication antenna which should be able to accept pointing errors of the order of some degrees.
In the following we assume that a maximum error of 2.5 degree is acceptable (semi conical angle).
Quite different is the problem posed by constraint on linear accelerations when translated in terms of angular rates and accelerations.

The requirement stated in the appendix D of the quarterly progress report #2 says that a max 1 degree uncertainty on the acceleration vector direction is allowable.
Even assuming that all the vector misdirection is due to attitude motion, this condition appears to be quite stringent (acceleration in direction orthogonal to the tether of the order of 2 hundredth of the residual gravity gradient acceleration). At very low acceleration levels (10^{-6} g = 1 μg) it is understood that larger values would be negotiable.

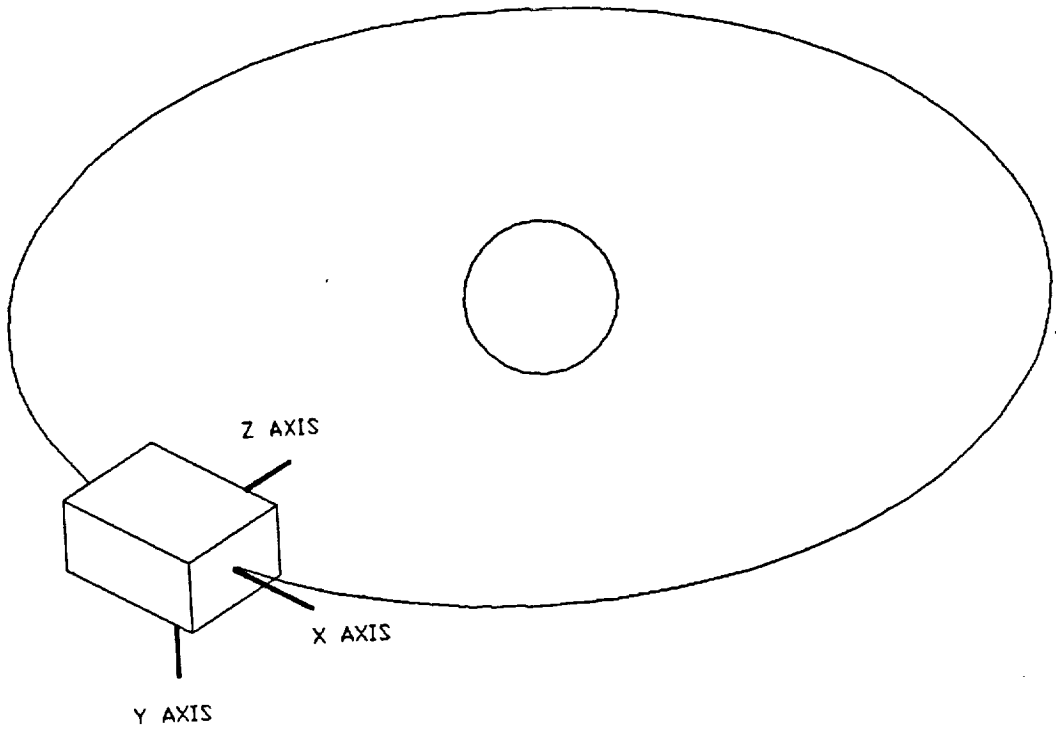

Fig. 2.1 - VGL reference frame

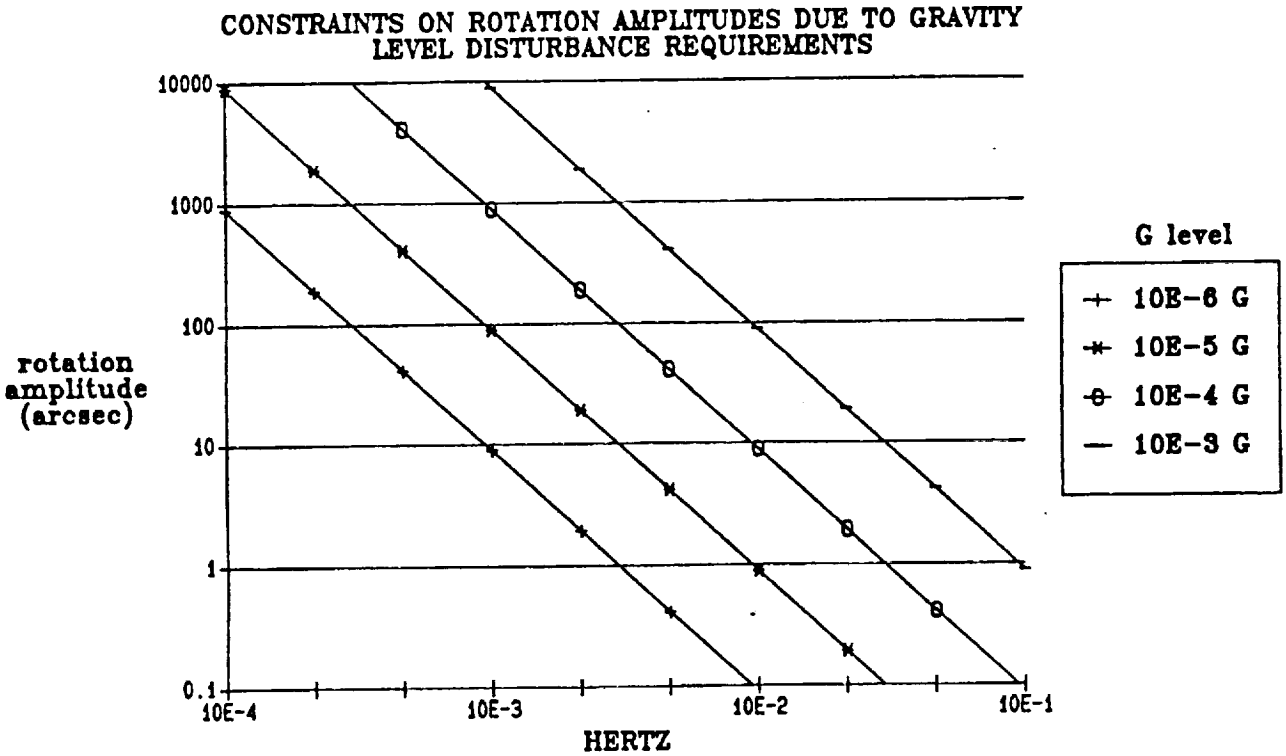

Fig. 2.2 Requirements on VGL attitude

For the pitch and roll axis the 1 degree requirement on the acceleration vector can be immediately translated in a max pointing error of 1 degree.
In case of a yaw axis pointing error there is a very small effect (due to the component of gravity gradient normal to the orbital plane). The max acceleration due to this is 0.3 μg for a point at 1 meter from the tether axis.

The pointing stability is a concern.
Rotations about the pitch, roll and yaw axes will cause centrifugal and tangential accelerations.
Admitting that the system is oscillating at a certain frequency f with amplitude δ the total acceleration is:

$$A = R \sqrt{[(\Omega^2 \delta \sin(\Omega t))^2 + ((\delta \Omega \cos(\Omega t))^2)^2]}$$

being

$$\Omega = 2 \pi f$$

R = distance between tether axis and point under consideration.

It can be shown that the max value of acceleration is either
$A = \Omega^2 \delta R$ = tangential acceleration
$A = (\Omega \delta)^2 R$ = centrifugal acceleration

The resulting max allowable δ as a function of the frequency f and of the residual gravity level is shown in fig. 2.2.
It can be seen how stringent the requirement becomes for the high frequencies
The bottom line is that relatively large value of mispointing are acceptable (expecially around the yaw axis) but only if a very slow motion is assumed.

2.3 EXTERNAL TORQUES

For external torques we mean all the torques acting on the VGL not due to the VGL control system.

2.3.1 Tether induced torques

The first torque to be examined and of paramount significance is the torque due to the tether itself. Obviously if the VGL is aligned with the reference frame no tether generated torque is present.
In case of pitch and/or roll motion the tension in the tether will cause a restoring torque on the VGL (for a generic motion of the VGL there will be also a net force on it which will bring back the VGL c.o.m. to a position along the local vertical for the Space Station c.o.m.).

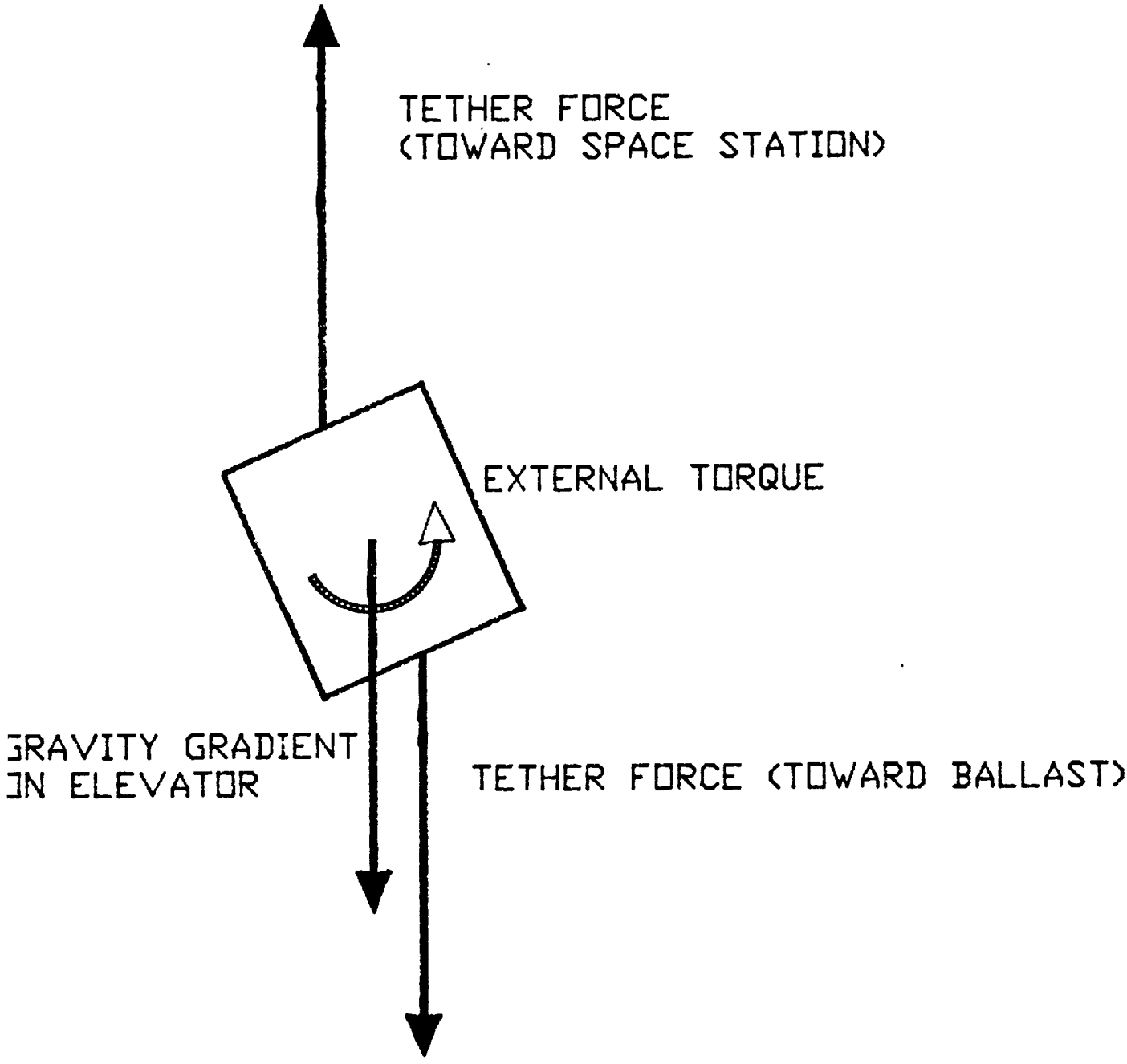

Fig. 2.3 - Forces and torques acting on VGL for a pitch motion

In a motion around the pitch axis, the tether portion between elevator and Space Station remains aligned with the local vertical for the overall c.o.m. whereas the tether portion between elevator and ballast is shifted (always parallel to the local vertical). See fig. 2.3.
The forces acting on the VGL are given by

F_b = tether tension at the contact point between VGL and tether toward the ballast

$$F_b = 3\ n^2\ [M_b\ X_b + 1/2\ \mu\ (X_b^2 - X_e^2)]$$

F_e = force acting on the VGL itself

$$F_e = 3\ n^2\ M_e\ X_e$$

F_s = tether tension at the contact point between VGL and tether toward the Space Station

$$F_s = F_e + F_b$$

with
M_b = ballast mass = 2200 Kg
M_e = elevator mass = 2000 Kg
X_b = ballast distance from overall c.o.m.
X_e = elevator distance from overall c.o.m.
μ = tether linear density ≈ 0.1 Kg/m

In fig. 2.4.a the stiffness of the VGL relative to a torque acting around pitch is reported as a function of the desired gravity level. This stiffness increases slightly with increasing length as, although the tether tension in the portion between the ballast and elevator decreases, the increase in the force acting on the VGL is rather large (in effect proportional to the gravity level).
For motion around the roll axis the problem is more complex as the out-of-plane gravity gradient plays a role. The response of system will tend to reduce to zero the displacement of the VGL c.o.m. and of the ballast as shown in fig. 2.5 . The displacement of these two point is quite small in any case (fig. 2.4.b) and is safe to assume that the roll stiffness is approximately equal to the pitch one.

Around the yaw axis the elastic properties of the tether come into play suppling a restoring torque in response to attitude disturbances (tether tension can not act around the tether axis if not through coupling effects between the motion around the principal axes of inertia).
The torsional stiffness of the tether is given by
$K = G\ Jp/l$
where

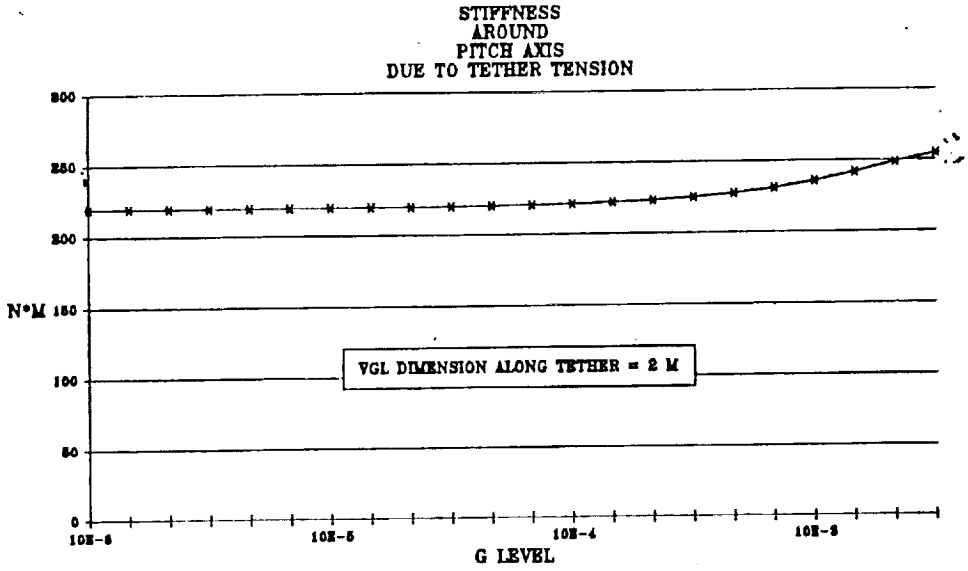

Fig. 2.4.a - Stiffness around pitch

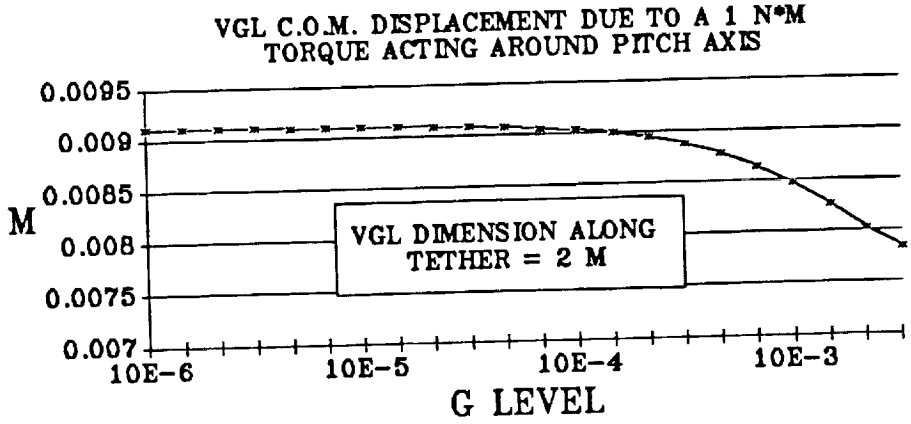

Fig. 2.4.b - Displacement of VGL c.o.m.

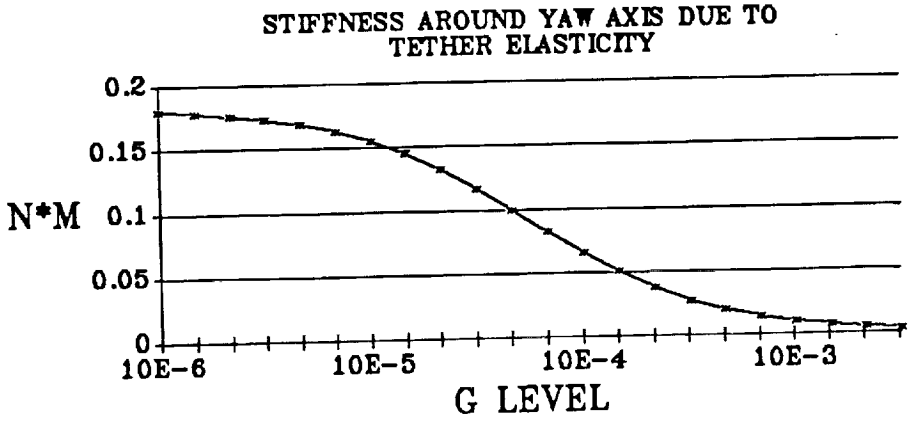

Fig. 2.4.c - Tether torsional stiffness

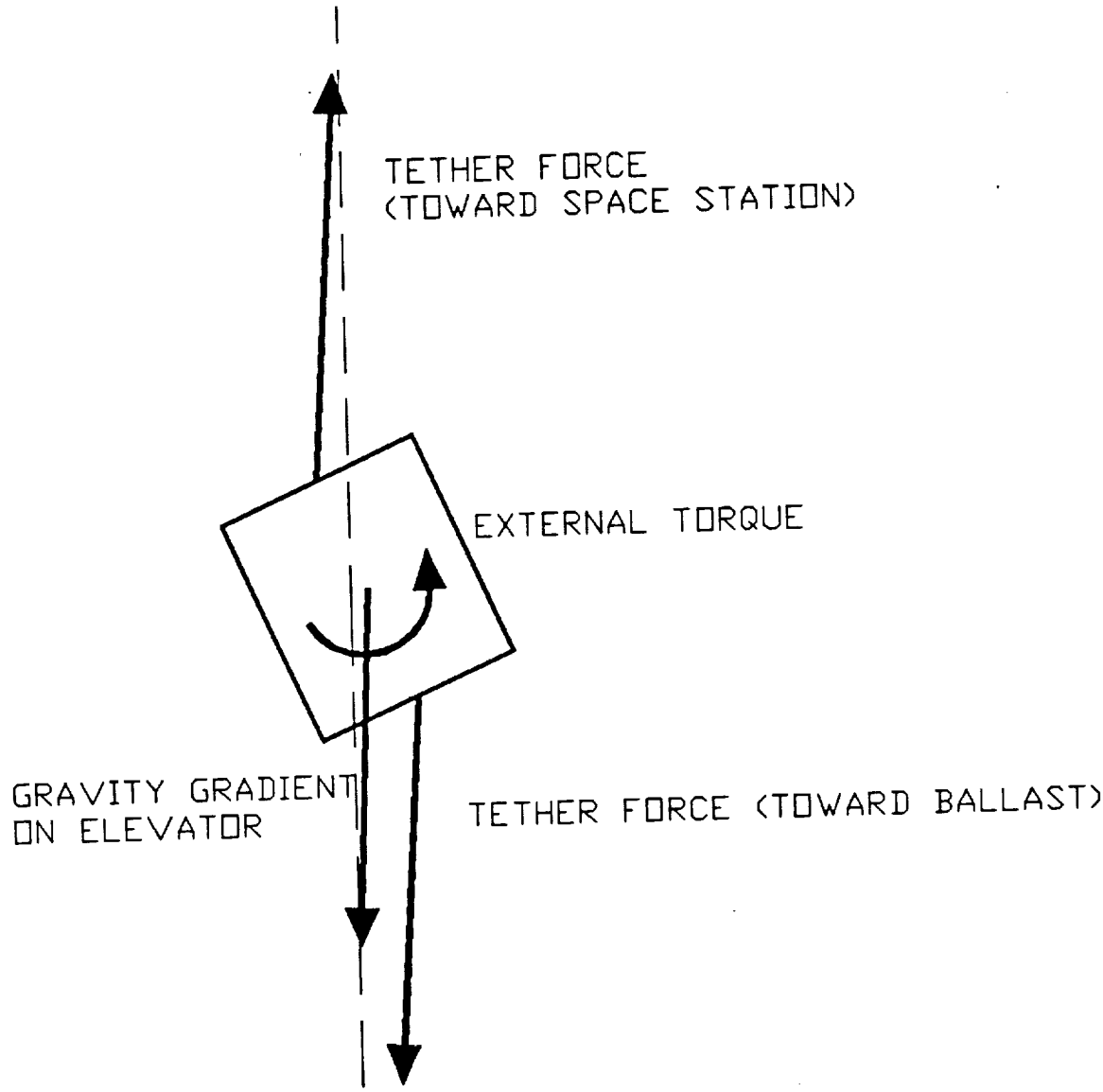

Fig. 2.5 - Forces and torques acting on VGL for a roll motion

G = transverse shear module = 26.3*10^9 Pa
Jp = polar moment of inertia of tether = 0.98*10^-9 m^4
l = tether length between elevator and Space Station.

The tether torsional stiffness is reported in fig. 2.4.c as a function of the VGL position.
It can be seen that there are at least three order of magnitude between the stiffness around pitch/roll axes and the one around yaw. This is important as it means that motion around the pitch and roll axis is driven by tether tension whereas around yaw other effects and actions can be significant.
Another important point to be underlined is the fact that VGL attitude motion around the pitch and roll axes is coupled with linear motion along the roll and pitch axes respectively.

2.3.2 Environmental torques

If the VGL is properly designed (that is with reasonable symmetry around yaw) the classic disturbances of aerodynamic drag and solar pressure should not be important. For instance if we assume that the center of aerodynamic pressure is 0.1 meter from the c.o.m. with an exposed surface of 1.5 m^2 the resultant yaw torque would be of the order of 10^-4 N*m which would cause a max yaw angle of 1 degree. The solar pressure effect is at least two order of magnitude lower. It has to be noticed that the spring-like behaviour of tether induced torques is particularly apt to control this kind of steady or quasi static disturbance torques. In any case, such large values of unbalance are unlikely in a system as the VGL which can tested and eventually modified in orbit.
Around the pitch and roll axes the much larger stiffness of the system due to the tether tension reduces the steady state errors to negligible values.
If the VGL c.o.m. is shifted from the tether there is a torque around pitch and roll which cause a static misalignment of the VGL axes from the reference frame. The entity of this misalignment is given in fig. 2.6 as a function of the gravity level assuming a c.o.m. shift of 0.1 m from the tether. It has to be noticed that for large values of the g level (that is when the elevator is quite near to the ballast) this misalignment is not negligible so a constraint on the maximum shift of the c.o.m. from the tether has to be imposed.
Magnetic effect can be cancelled out with a proper design. Notice that the magnetic field will be in any case distorted by the Space Station itself.

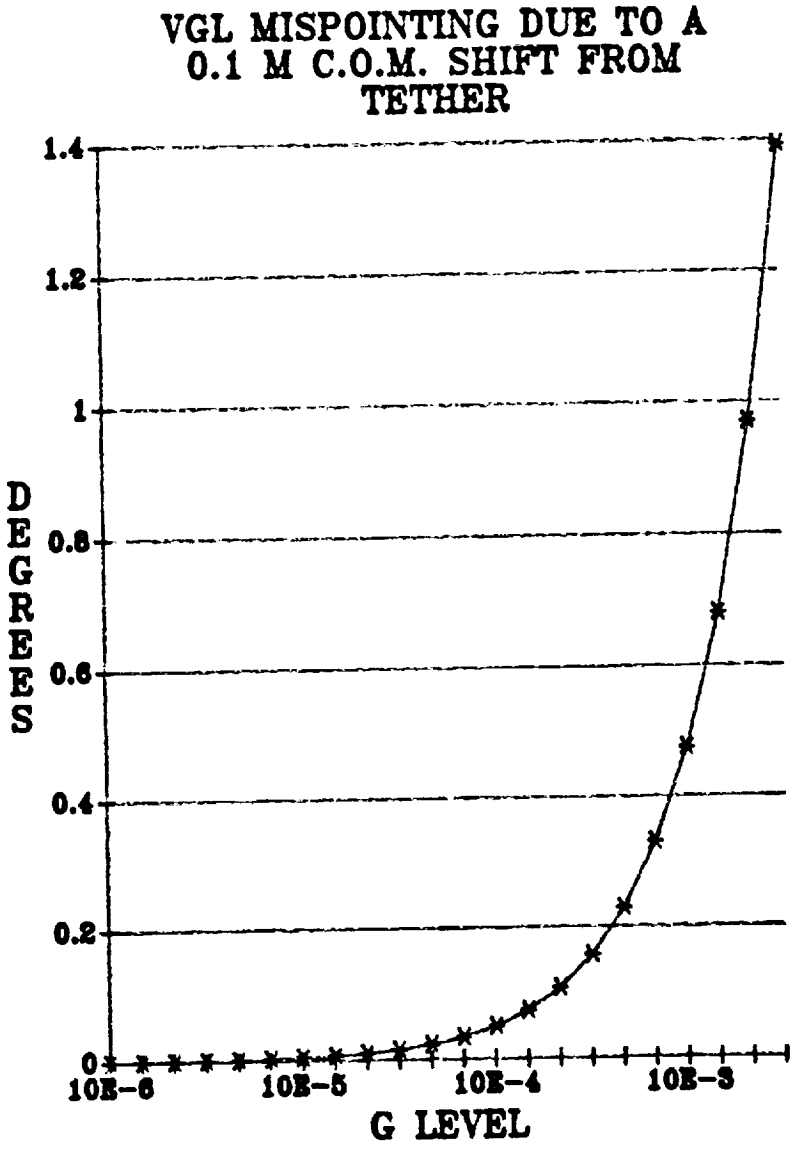

Fig. 2.6 - VGL mispointing due to c.o.m. mispositioning

2.3.3 Transfer motion induced torques

The VGL motion along the tether will cause attitude motion of the VGL around the pitch axis due to the Coriolis force and to the coupling between linear and angular displacements. This is not worrisome as long no experiments will be performed during the VGL motion. Residual vibrations can possibly be a cause of concern which can be evaluated only when simulation results will be available. As an educate guess we feel confident that the tether tension will restrain these motions within acceptable limits. In any case damping can be provided using proper actuators.
An important constraint has to be met regarding the alignment of the principal axis of inertia with the roll and pitch axis. If this is not so, the coupling with the motion around the yaw axis which would occur, would cause motions around the yaw axis not easily controlled by the tether itself

2.3.4 Docking torques

A special case of attitude control will occur when the VGL is very near to the Space Station. In general it will be necessary to rotate the VGL around the yaw axis to accomplish the nominal docking position. At short length the cable torsional stiffness is quite high . For instance if the tether length is 1 meter and the required rotation is 5 degree a torque of 2.25 N m would be required. In effect the VGL is not rigidly mated with the tether but exchange with it contact forces through friction. So the tether can react to torques on the VGL only up to a certain value dictated by the friction.
For instance near the Space Station a longitudinal force of 1 N is sufficient to stop the VGL. With a tether radius of 0.01 m a torque exceeding 5*10^-3 N m will cause slippage between tether and VGL. This is not necessarily a drawback as it permits large rotation of the VGL with a small torque applied.

2.4 ACS EQUIPMENT

Only a tentative description of the ACS can be given at this stage.

2.4.1 ACS sensors

In general for the ACS it will be necessary to measure the attitude of the VGL and receive information on its position (given that attitude torques and linear motions of the VGL are coupled through tether and gravity gradient).
The position of the VGL with reference to the overall c.o.m. can be reconstructed using the in board accelerometers. The position of the VGL with reference to the the

Space Station should be measured independently using, for instance, a Space Station based ranging and tracking laser with corner reflectors on the VGL. Notice that the position of the VGL w.r.t. the Space Station is different from the travelled tether length if the tether is arched.
Although the system for the acquisition of the VGL position is not part of the ACS some ideas on it potential capabilities and implementation are given here. The travelled tether length and eventually the travelling speed should be measured on the VGL itself; this should be easy it the wheel speed is measured.
Measures of three axial accelerations are needed for the experiment history reconstruction. These measures will be used to supplement the information on the relative position of VGL and Space Station but might not be sufficient as too many sources can contribute to the accelerations and only scant information can be deduced for the motion along the flight direction.
The information on the position of the VGL on the tether and relative to Space Station will be used to command VGL motion along tether itself.

The main sensors for the VGL attitude will be rate gyros updated by a combination of a sun sensor (or star sensor) looking along the flight direction and a star sensor looking in the out of plane direction. The use of an Earth sensor (horizon sensor) is not thought advisable as occultation problems due to the Space Station are foreseen; the line of sight along the local vertical can be precluded by the ballast. The likely distortions in the magnetic field due to the Space Station itself preclude the use of a magnetometer.
Due to the relative short duration of the mission the orbital precession should be small enough to permit the use of a single star sensor which updates the gyros once per orbit.

2.4.2 ACS actuators

The main problem on the ACS equipment is the kind of actuators which should be used. In particular the problem is whether reactions wheels are needed. Cold gas thruster will be in any case needed either to desaturate the reaction wheel or to directly assuring attitude control; the use of hydrazine is not advisable to avoid problems with the gas plume impingements. At this point of the analysis it would be unwise to search a definitive solution. We could point to the main issues which weighs on the choice the attitude control actuators:

a) For motions around the pitch and roll axes the reaction wheels are not deemed necessary as the degree of stabilization that the tether tension can supply seem sufficient. The damping of these motions can eventually

require them, but any attempt to counter the tether tension generated torque would easily surpass the wheels capacity. A passive oscillation damper is an additional device which should reduce efficiently the rather quick oscillations around the pitch and roll axes. Notice that contrarily to ordinary satellite the VGL has an intrinsic capability to damp momentum exchanging torques with the tether.

b) The degree of stabilization offered by the tether around the yaw axis is relatively low expecially far away from the Space Station. The reaction wheel offers the capability of controlling this motion but they require in any case some device to damp their momentum.

c) Reaction wheels are in general rather bulky and noisy (this point is particularly important for the very low g VGL mission phases) but their action can be controlled in a continuous fashion.

d) Gas jets have a lower limit on the resolution of the torque and momentum which they supply giving place to a limit cycle motion. Beside they also consume propellant, but as the VGL is easily resupplied this is not a concern.

In substance the design philosophy of ACS should be the following:

- Passive oscillation dampers act around the pitch and roll axes with the tether tension playing the main role in the attitude control. Cold gas jets use is suggested if exceedingly high momentum damping requirement are foreseen (this can happen for instance at the end of large VGL transfer motion).

- Around yaw only cold gas jets and passive dampers should be used if possible. The torsional stiffness of the tether should be sufficient to control yaw oscillations expecially at low g level when the tether is quite short even if the requirements are more strict. Reaction wheels are necessary if yaw motions (deduced by computer simulations) are expected to be fairly large and/or the control capability of the gas jets is deemed unsatisfactory

2.5 ANALYSIS SUMMARY

It was shown that the ACS requirements come mainly from the VGL gravity level requirement.
The main torques acting on the VGL are those due to the tether itself expecially around the pitch and roll axes. Coupling occurs between attitude and position of the VGL. Simulation results are needed to assess correctly the

Attitude and position control of the VGL requires a set of sensors including gyros and star/sun sensors for the attitude and accelerometers, possibly a laser ranging/tracking system on the Space Station and devices able to measure the travelled tether length and speed.
The restoring torques due to the tether coupled with damping devices are deemed sufficient to control the attitude around pitch and roll axes. Cold gas jets can be used to damp exceedingly large oscillations.
The torques around yaw can be controlled only to a limited degree by the tether torsional stiffness. Cold gas jets can be used, but their effectiveness is hindered by their finite resolution in terms of torque and momentum. If large torques are present or exceedingly long settling times are foreseen on the basis of simulation results a yaw reaction wheel should be adopted.

3. CONFIGURATION CONSTRAINTS

The VGL configuration and subsystems are deeply influenced and in some case driven by the constraint imposed by the VGL mission itself. A preliminary categorisation of these constraints and an estimate of their relative weight are deemed necessary prior to the proper configuration identification.

3.1 G LEVEL

The most distinguishing feature of the VGL is its capability of achieving various static levels of acceleration (comprehending a near zero level). This feature has an important effect on many subsystem

- The structure should be such to transmit the lowest possible disturbances from the tether to the payload.

- The thermal, power and ACS subsystem should be built with the fewest possible moving components in order to avoid uncertainties on the location of the VGL c.o.m. and mechanical noise due to dynamic effects.

- The non zero gravity can alter the nominal behaviour of some components. This is particularly true for equipments involving fluid transfer as for instance heat pipes.

- The mechanism for VGL translation along tether should be able to supply the required, variable force along tether and pressure on the tether itself.

3.2 ACCESS

The VGL is made as a refurbishable, reparable system. This implies that access should be guaranteed to as many equipments as possible. Two subsystems in particular are required to be easy accessible:

- The mechanism responsible for VGL translations along tether, which is rather complex and critical. Visual inspection possibility and access have to be guaranteed at all times.

- The power subsystem, if based on batteries power, should allow easy replacement of the batteries in a flexible way. The batteries replacement will take place on the Station on its immediate proximity with the VGL being not operative, so this problem should be solvable.

3.3 PAYLOAD REPLACEMENT

The VGL payload changes from mission to mission and there is not a baseline payload to which one can refer to.
To make easy payload replacement a modular concept is the best choice.
In any case the capability of changing payload has an influence on many subsystem. In fact:

- The structure must be able to accommodate one or more module containing the payload, in a position as near as possible to c.o.m. of the VGL (which is presumably near to the geometrical center of the VGL).

- Thermal control, power and data handling subsystems should be able to interface with the payload in a standardised and flexible fashion. This should be relatively easy for the power and data handling, involving only electrical connectors but can be difficult for the thermal control subsystem where physical contact is required.

- The ACS is influenced by the mass properties of the payload. This implies on one hand constraints on the allowable mass properties of the payload, on the other hand requirements on the ability of the ACS to deal with a set of possible mass properties of the VGL.

- Opportune mechanical interfaces and mechanisms must be provided to permit easy replacement of the payload.

3.4 SURFACE CONSTRAINTS

In order to reduce the structural flexibility of the VGL no wings of solar arrays nor of thermal radiators are foreseen.
In this way the amount of external surface available to the power and thermal control subsystems is limited leading to a specialized design.

3.5 SLOT CONFIGURATION

The design decision leading to a slot configuration (see appendix A chapter 1 of progress report #5) is a driver for:

- Structure. The general shape of the structure is almost completely dictated by the slot presence.

- Mechanism. The mechanism used for VGL motion along tether should be able to engage and disengage from a tether which is entered in the VGL through the slot.

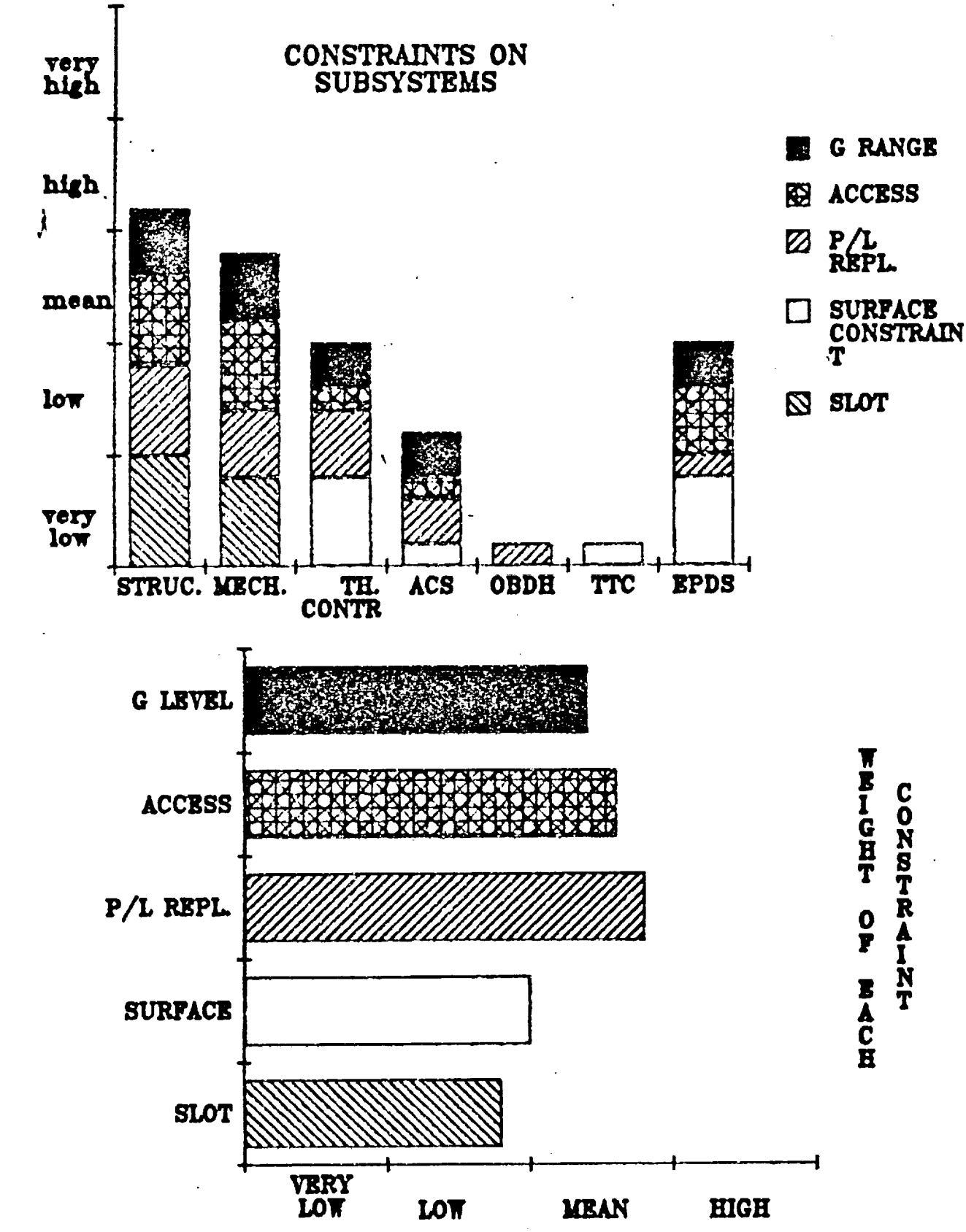

Fig. 3.1 - VGL configuration constraint

3.6 SUMMARY

A pictorial summary of the analysis on the configuration is reported in fig. 3.1. A relative weight (from very low to very high) was assigned to each constraint to give an idea of what we feel to be important for each subsystem. Some items of this evaluation can be not apparent from the above discussion:

- The thermal control and the ACS subsystems need a certain degree of accessibility. The thermal control can require some reconfiguration when the P/L is changed and there is the need of resuppling attitude control cold gas jets.

- The TT&C system requires a certain amount of surface (or more correctly Space Station visibility).

- The star/sun sensors of the ACS require an unimpeded field of view.

It can be seen that the structure is singled out as the most constrained subsystem, which is another way of saying that the structure depends strictly on the unique mission concept the VGL.
The other subsystems which are critical are the thermal control, power and mechanism. The ACS does show some problems whereas the TT&C and the OBDH appear quite standard design.
The lower graph shows what is the order of importance among the various constraints on the VGL design. It is noticeable that the most important constraint is the VGL ability to replace payload.

4. PAYLOAD

As shown in the previous section the problem of replacing the payload is of paramount importance to the VGL conceptual design. So in the following an outline of the payload problems is made and design decisions are suggested.

4.1 PAYLOAD LOCATION AND SIZE

The payload location and size are almost completely determined by the condition of achieving a max value of 10^{-6} g (= 1μg) all over the payload when the VGL is on the c.o.m. of the whole system.
In the following discussion reference will be made to the VGL S/C that is the VGL without the payload.
The gravity gradient acceleration is given by

$$a_x = 0$$

$$a_y = -n^2 y$$

$$a_z = 3\, n^2 z$$

n = mean orbital motion = $1.14*10^{-3}$ sec^{-1}

So the volume into which the gravity gradient is less than 10^{-6} g is an a elliptical cylinder with the semi mayor axis being a = 7.5 m and semi minor axis b = 2.5 m. The center of the ellipse is on the overall c.o.m.
The desired level of 1 μg can then be obtained keeping the payload and overall c.o.m. as near as possible with all the payload located within the above mentioned envelope (as a maximum) .
It is possible to think to a system where the payload c.o.m. does not coincide with the VGL S/C one, but that would make things more complex as the payload mass is different for each VGL mission; the VGL c.o.m. would change increasing difficulties in the design of the ACS and in the determination of the desired nominal position of the VGL.
So the baseline choice is that the payload and VGL S/C c.o.m. coincide. This implies that the payload has to be located in position which is somewhat within the VGL.

Apparently there is ample room for the payload. In reality there are other accelerations to be included if one wants meaningful results.
First of all there is the acceleration due to aerodynamic drag which is of the order of 0.3 μg.
Accelerations due to the attitude motions are more difficult to assess. We can say that they increase linearly

value can be obtained only after thorough analysis and simulations.
We can assume, for the sake of simplicity that the acceleration along the three axes are given by

$a_x = -a_d + a_a\ x$

$a_y = -(n^2+a_a)\ y$

$a_z = (3\ n^2+a_a)\ z$

where

a_d = drag acceleration

a_a = acceleration due to attitude motion for a point at 1 m from the c.o.m.

Depending on the sign of the acceleration due to attitude and due to the presence of the drag constant acceleration the ellipsoid representing the zone within 1 µg is shifted forward and backward along the X direction.
In fig. 4.1.a ,4.1.b and 4.1.c the intersection of these ellipsoids with the planes x = 0 and y = 0 is pictured in the worst case for various level of the acceleration due to attitude motions.

In the following table the max distances at which a point may be, still meeting the 1 µg requirement

a_a at 1 m	X	Y	Z
0.10 µg	7.0 m	4.1 m	1.9 m
0.20 µg	3.5 m	2.9 m	1.6 m
0.30 µg	2.3 m	2.2 m	1.4 m
0.40 µg	1.7 m	1.8 m	1.2 m
0.50 µg	1.4 m	1.5 m	1.1 m
0.60 µg	1.2 m	1.3 m	.96 m

Table 4.1

On top of the attitude disturbances other noise sources should be considered as longitudinal tether vibration, mispositioning of the VGL on the tether, pendulum - like tether motion which act mainly along the tether direction.

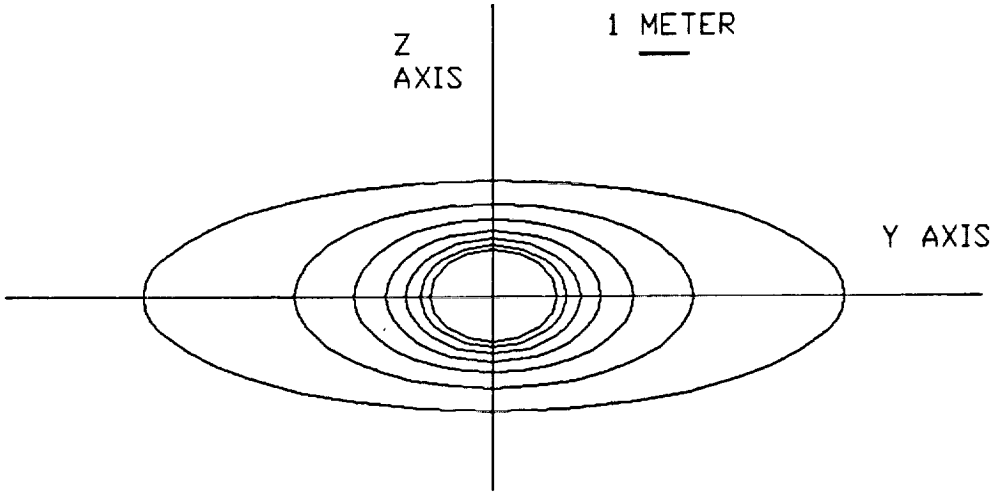

Fig. 4.1.a - YZ plane

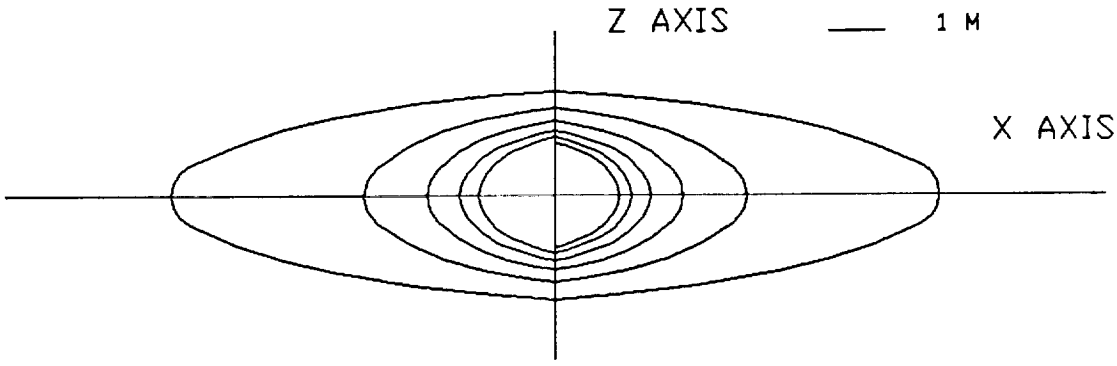

Fig. 4.1.b - XZ plane

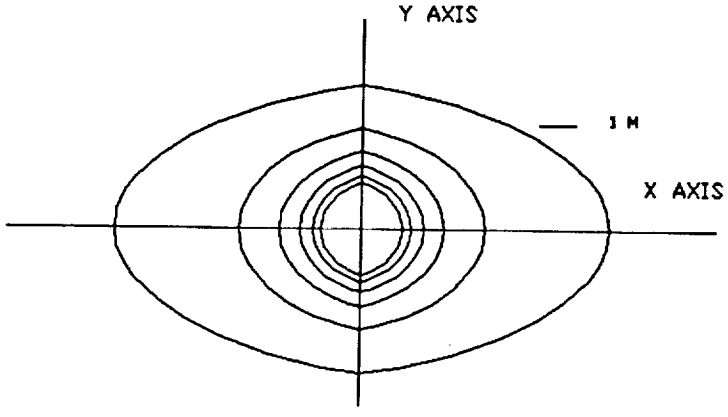

Fig. 4.1.c - XY plane
Fig. 4.1 - 1 µg zone for various levels of a_a
(from 0.1 to 0.6 µg at 1 m)

a_a at 1 m	X	Y	Z
0.10 µg	7.0 m	4.1 m	1.7 m
0.20 µg	3.5 m	2.9 m	1.4 m
0.30 µg	2.3 m	2.2 m	1.2 m
0.40 µg	1.7 m	1.8 m	1.1 m
0.50 µg	1.4 m	1.5 m	1.0 m
0.60 µg	1.2 m	1.3 m	.86 m

Table 4.2.a - acceleration along z = 0.1 µg

a_a at 1 m	X	Y	Z
0.10 µg	6.6 m	3.9 m	1.3 m
0.20 µg	3.3 m	2.7 m	1.1 m
0.30 µg	2.2 m	2.1 m	.94 m
0.40 µg	1.6 m	1.7 m	.82 m
0.50 µg	1.3 m	1.4 m	.73 m
0.60 µg	1.1 m	1.2 m	.66 m

Table 4.2.b - acceleration along z = 0.3 µg

a_a at 1 m	X	Y	Z
0.10 µg	5.7 m	3.5 m	.91 m
0.20 µg	2.8 m	2.4 m	.76 m
0.30 µg	1.9 m	1.9 m	.65 m
0.40 µg	1.4 m	1.5 m	.57 m
0.50 µg	1.1 m	1.3 m	.51 m
0.60 µg	.94 m	1.1 m	.45 m

Table 4.2.c - acceleration along z = 0.5µg
Table 4.2 - 1 µg zone for various levels of a_a and along z

Parametrically changing the value of this "steady" disturbance along z we obtain the results reported in table 4.2,4.3 and 4.4. They say that the space available along the z direction is approx 2 m and somewhat more (2.5 to 3.5 m) in the other two directions.
Other considerations reduce the amount of space available. It is reasonable that a 0.25 m radius zone around the tether is negated to the payload and further space is taken away for the presence of the slot.

What is the amount of space that we reasonably need for the payload?
This is rather difficult to say but as a guideline we can assume a packaging density between 0.1 and 0.3 (Kg/m^3). For a payload mass between 500 and 1000 Kg this results in something between 1.6 and 10 m^3 with a reasonable value of 4 m^3 as baseline (geometrical average).

Leading dimensions of the payload would be then

x = 2 m

y = 1.8 m

z = 1.5 m

4.2 PAYLOAD CONFIGURATION

Basically two choice are available for the payload conceptual configuration: payload racks or payload module

In the first solution there is a set of racks on the VGL each able to house relatively small experiments separately. As most of the scientific activity will involve the processing of identical samples at various g - levels this choice has some merit.
From the VGL point of view this implies the presence of multiple interfaces between the VGL and the payload which is obviously burdensome. Another drawback is the fact that standardization of the racks reduces the flexibility of the system (only experiment up to a certain size may be housed).
The payload module solution foresees a single large module which can be mounted on the VGL as a whole and has a single interface with the VGL. The main advantage of this solution relies just in this interface simplification. The flexibility of the system is increased as the constraint on the size of the experiments is greatly relaxed. Another point worth notice is the fact that if the VGL mission is used for a single set of experiments the payload module

can be specialized to a large degree with an increase on the mass and volume efficiency. From the operational point of view the payload module require the same amount of operation which would be required for a single experiment rack; on the other hand the payload module would be a rather bulky object when compared to the single rack experiment, making each operation more complex (notice that eventually the payload module can be made by two or three sections). The interface with the VGL thermal control subsystem appears very difficult if fluid transfer is required. Right now, the best solution appears to be the one in which the payload module is able to handle its thermal control using the VGL only as a shield and power source for the heaters. Possibly there can be a cold plate on the VGL which can act up to a certain point as an heat sink for the payload. In this way the VGL thermal control subsystem can be kept simple avoiding overdesign in the effort of dealing with all the possible situations. As last point it has to be said that the payload module can eventually be configured (if the need arise) as a removable rack offering a compromise between the two solutions.
Weighting the relative merit of each solution it was decided that the payload module configuration offers the best potential for exploiting the VGL capabilities.

5.0 ACCELERATIONS MEASUREMENT ON VGL

The experiments mounted on VGL as well as the manoeuvres of positioning of the elevator along the tether require an accurate measurement of the acceleration occurring on board the VGL itself.
In this chapter we define a set of requirements for the accelerometers, and discuss the principal problems, and some possible solutions, related to the measurements of the acceleration environment, in view of the results of a preliminary review of existing accelerometers.

5.1 UPDATED REQUIREMENTS FOR THE VGL ACCELEROMETERS

The microgravity environment of the VGL is characterised by accelerations ranging between about 10^{-8} and 5×10^{-3} g in amplitude, and from 0 to 100 Hz in frequency.
Acceleration sources at very low frequencies (0 - 0.01 Hz) are the gravity gradient, atmospheric drag, orbital perturbations, tether oscillations, and the VGL motion along the tether. The main microgravity disturbances occurring in the higher frequency band are still object of theoretical investigation. Nevertheless, it is very likely that perturbing accelerations occurring in the band 1 - 100 Hz are caused by running machinery and by the motion of mechanical parts (valves, switches, etc.), while those in the intermediate range (0.01 - 1 Hz) are due to the VGL attitude motion and, partially, to the tether oscillations induced by the elevator motion. The foreseen envelopes in amplitude and frequency of the accelerations acting on the VGL, during a mission in which the elevator is positioned successively at the various gravity levels (from 10^{-6} g to 0.4×10^{-2} g), are shown in fig. 5.1.

By considering the experiments requirements concerning VGL residual acceleration features and monitoring in range, frequency, accuracy (ref. LOW GRAVITY PROCESS IDENTIFICATION, Final Report, February 1989) together with the foreseen microgravity environment, it turns out that the required monitoring will be guaranteed by sensors able to measure accelerations along the three VGL axes in the bandwidth 0 to 100 Hz, ranging from $\pm10^{-2}$ g, and with an accuracy plot as shown in fig. 1. Of course, these same accelerometers will be suitable also for supporting the elevator positioning along the tether at required micro-g levels.

In order to be certain that the sensor is suitable for detecting the anticipated signal, its theoretical limit of resolution (or sensitivity), i.e. its intrinsic noise, must be lower than the smallest acceleration to be measured. In particular the sensor resolution is usually chosen to be an order of magnitude below the smallest

signal at any given frequency; this, in our case, implies an internal noise with spectral density not greater than 10^{-10} g/$\sqrt{Hz}$ in the frequency range 0 - 100 Hz.
In fact, if the instrument has the abovementioned noise, flat from 0 to 100 Hz, its resolution (rms noise power) on that bandwidth turns out to be:

$$\left[\int_0^{100} 10^{-20} \, df \right]^{1/2} = 10^{-9} \text{ g} ,$$

a value which is 10 times lower than the lowest signal (10^{-8} g) that should be measured by the accelerometer in the that given frequency band.

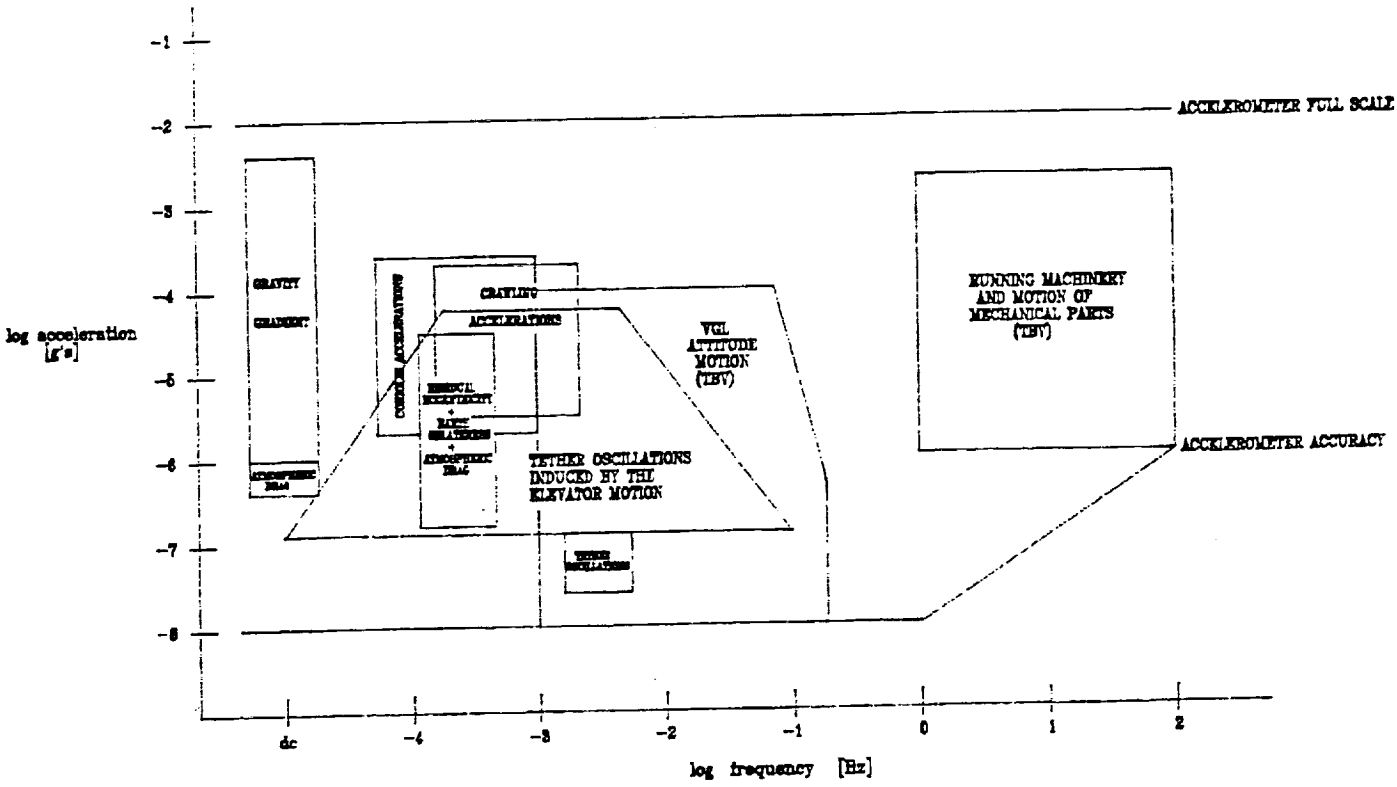

Fig. 5.1 - VGL accelerations envelopes and accelerometers package accuracy plot as function of the frequency.

The requirements on the VGL accelerations measurement should
be therefore completely fulfilled by an accelerometers package having the following characteristics:

MEASUREMENT RANGE	-10^{-2} g to $+10^{-2}$ g
FREQUENCY BAND	dc to 100 Hz
MEASUREMENT ACCURACY	10^{-8} g from dc to 1 Hz, and not exceeding a matched linear increase with frequency, up to 100 Hz
RESOLUTION	10^{-9} g (for sensors operating in the whole frequency band 0 - 100 Hz).

The acquisition of high quality data during long periods of time, like the duration of the typical VGL mission (about 1 month), requires moreover that the accelerometers have good bias stability and low time-dependent drift and temperature coefficient of the bias.
The possibility of on-orbit calibration, an high degree of linearity in both the amplitude and frequency ranges, and a short thermal/mechanical stabilisation time are also very desirable features.
Precise upper limits on the mass, size, power will be assigned once the overall configuration of the VGL as well as a preliminary mass and power breakdown among its subsystems will be defined; nevertheless, at this time, they don't seem to be critical parameters for the accelerometers selection.

During any mission of the VGL it is required, in addition, the knowledge of the frequency spectrum of the accelerations environment for the following reasons:

- to monitor the value of the (quasi-)steady component of the acceleration (those generated by gravity gradient) during the elevator motion along the tether for its correct positioning to the desired micro-g level,

- to verify that the required profile of the residual acceleration as function of the frequency (ref. fig. 3.1 of progress report #5) has been maintained during the experiments activity.

The selected sensor(s) must therefore be interfaced with a Data Acquisition System and a Data Reduction System suitable to provide the required information about the signal spectrum; in particular the sampling rate must be at least twice the maximum frequency to be detected. In addition the information about the steady component of the

used to support the positioning operations.

5.2 RESULTS OF THE PRELIMINARY RESEARCH ABOUT ACCELEROMETERS

A preliminary research has been performed aimed to collect documentation about the technical characteristics of existing accelerometers, to be used as a basis for a successive selection of sensors suitable for applications on board the VGL.
The accelerometers considered have been divided in two categories:

- accelerometers currently available for space applications,
- accelerometer under study or development, exploiting both conventional and new technologies.

Within the present section we describe only sensors whose performances (full scale, bandwidth, resolution) keep close to the required performances, defined in the previous paragraph.

5.2.1 Currently Available Sensors

Among the accelerometers designed for low-g space applications, the MESA is the most proved and space qualified piece of hardware.
This sensor is built by the Bell Aerospace Textron and consist of a proof mass (a thin walled flanged cylinder) electrostatically suspended in all three axes, i.e., when it is in operation, there is absolutely no physical contact between the proof mass and any other part of the accelerometer. The electrostatically suspension, with respect to the mechanical one (springs, etc.), has the advantage of reducing the bias instability, the time-dependent drift, and the bias temperature coefficient.
This sensor is available in both single-axix and three-axis version. Approximately 40 single-axis and 9 three-axis MESAs has been built and flown on several satellites and on the Space Shuttle.
The main characteristics of MESA accelerometer are given below.

Full Scale	$\pm 10^{-3}$ g to $\pm 2.5 \times 10^{-2}$ g typically
Frequency Band	0 to 10 Hz (an exception is the MESA which flown on Spacelab 3, and whose bandwidth was 50 Hz)
Sensitivity	10^{-8} g

Size	9x13x10 cm
Mass	3 kg
Power Required	15-20 W

Most of the power goes into the oven heaters, needed for the provision of a temperature controlled environment, and therefore it is not a continuous requirement after the system reaches the operating temperature.
The MESA can be provided with multiple sensitivity ranges and with an autoranging circuitry able to select the most appropriate range for the input signal.

Another three-axis accelerometer based on the same principles of operation of the MESA, but using a spherical proof mass, is the French ONERA-built CACTUS.
It has been designed especially for very high precision measurements of the perturbation forces due to air drag and radiation pressure from the Sun and the Earth, and flown on the CASTOR-D5B satellite in the 1975.
CACTUS has a full scale of $\pm 10^{-5}$ g and a resolution of about 10^{-11} g.

Among the accelerometers with a bandwidth including the range 10-100 Hz, the Q-flex, built by Sundstrand, is the sensor whose global performances are closest to our requirements. It is a single-axis accelerometer, consisting of a test mass on a quartz hinge (the force rebalance is provided by a coil on the hinge) and it has been used for the inertial navigation.
Main characteristics:

Full Scale	± 3 g max
Frequency Band	0 to 600 Hz
Sensitivity	10^{-6} g
Size	2.5x2.5 (diameter) cm
Mass	0.08 Kg
Power Required	0.3 W

Sundstrand engineers feel that the sensor could provide meaningful information also at 10^{-7} g if a few changes were made, including the provision of a temperature-controlled environment.

5.2.2 Accelerometers Under Development

In the 1986 the Bell Aerospace Textron started the development of an improved version of the MESA. This new instrument uses a cubic proof mass (electrostatically suspended) in place of the flanged cylinder, thus providing constrainment against six degrees of freedom instead than five. As a consequence the sensor can measure both linear accelerations along three axes and angular accelerations around three axes. The preliminary specifications for the Cube Proof Mass MESA are given below.

Full Scale	$\pm 10^{-5}$ g (lowest range) $\pm 10^{-2}$ g (highest range)
Ranges Available	3 from 10^{-2} to 10^{-5}
Sensitivity	10^{-9} g
Size	9x13x23 cm
Mass	2.27 kg
Power Required	9 W
Operating Temperature	-23° C to +71° C

Other remarkable features which should characterise this accelerometer are high bias stability, an high linearity, and the possibility of being calibrated in 1g ground environment, and of withstanding accelerations up to 15 g in nonoperating mode.

The most sensitive accelerometers under development for space applications are those projected for satellite gravity gradiometry.
To this class it belongs the GRADIO, improved version of CACTUS, which is based again on a cubic proof mass electrostatically suspended. This instrument should be characterised by a full scale of $\pm 10^{-5}$ g and a theoretical resolution 10^{-13} g/$\sqrt{Hz}$, together with an high linearity and high bias stability.

Another sensor with performances similar to the GRADIO ones, is the superconducting six-axis accelerometer, developed at the University of Maryland for application in gravitational wave detection and gravity gradiometry. The accelerometer is composed of a magnetically levitated superconducting proof mass, a superconducting magnetic transducer and a low noise superconducting magnetometer, called "SQUID" (Superconducting Quantum Interference Device). The magnetic field produced by the transducer

detected by the SQUID magnetometer. This instrument requires a dewar with liquid Helium for its thermal control, as it has to operate at cryogenic temperature. A reduced scale prototype single-axis gradiometer has been assembled and tested. Experimentally, noise levels of about 7×10^{-11} g/$\sqrt{Hz}$ in a frequency windows between 0.1 Hz and 1 Hz, and an upper limit of 3×10^{-11} g/$\sqrt{Hz}$ around 15 Hz have been observed.

Among the sensors based on new technologies those that seems the most promising for meeting performance goals required by VGL are the solid state accelerometers and the optical cavity looking accelerometers.

Accelerometers of the first kind are the Integrated Silicon Accelerometer (ISA), under development at Honeywell, and the solid state accelerometer developed by Centre Suisse d'Electronique et de Microtechnique (CSEM) under ESA contract.
An important feature of integrated sensors is that the signal conditioning electronics is realised on the same silicon chip as the transducer. As a consequence these sensors are less vulnerable to noise and leakage than discrete ones. In addition the package size, weight and power consumption of solid state accelerometers are considerably smaller than those of the other sensors. Sensitivities between 10^{-7} g and 10^{-6} g, together with frequency range of few hundred Hz starting from dc, and dynamic range larger than 10^{6} were obtained with breadboarded sensors of maximum size 5.4x4x1.6 mm. It was also shown that the limits in performance were not reached, and that considerable improvements in sensitivity and bandpass might be envisaged.

The operational principle of the Cavity Looking Accelerometer (CLA), projected by Honeywell, is based on tracking the resonance frequency of an optical (Fabry-Perot type) cavity.
A laser beam is injected into the cavity and the transmitted output is measured by a photodetector. The strategy in the CLA is to assure that the frequency of the probe beam matches a resonance frequency of the interferometer cavity at all times. Accelerations along the cavity axis are therefore detected as they induce a chance in the cavity length which disturbs the resonance condition.
A sensitivity analysis for the CLA shows that this kind of accelerometer can reach a resolution of about 10^{-9} g. The maximum acceleration that the CLA can measure depends on the particular scheme of its frequency tracking; signals of some tens of g's in amplitude seems within the capabilities of this accelerometer.

of the abovementioned accelerometers are reported in fig. 5.2 and 5.3, superimposed to the region of the acceleration-frequency plane defined by the required range, bandwidth, and resolution; vertical broken lines are used in those cases in which the sensor bandwidth is unknown.

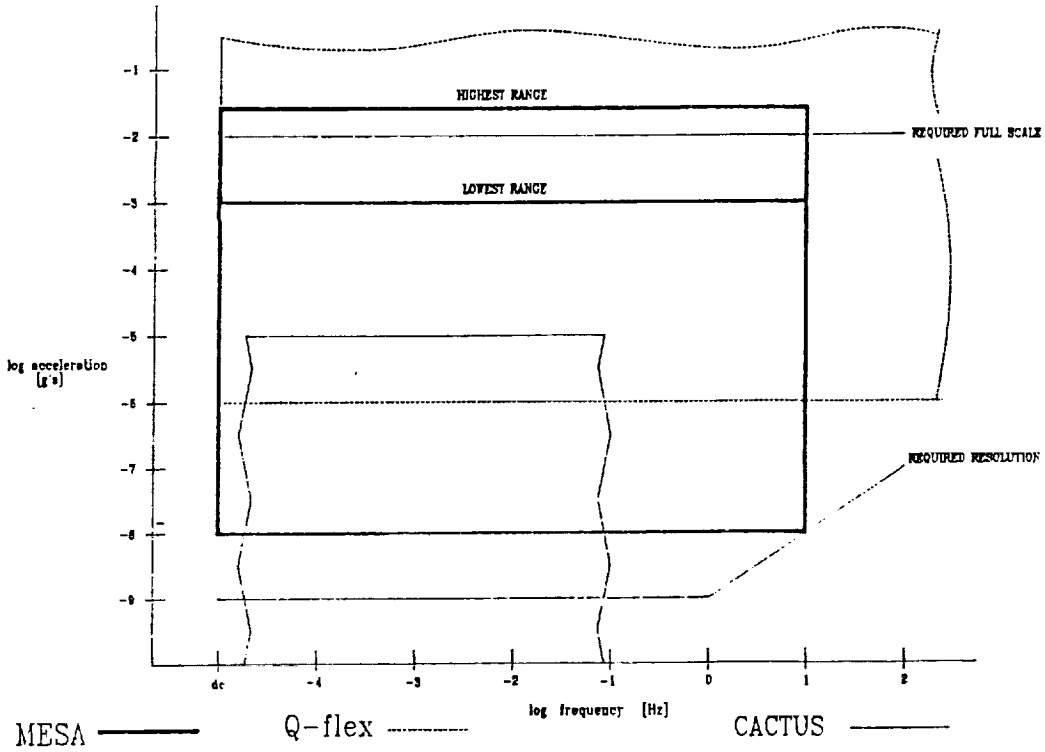

Fig. 5.2 - Full scale, bandwidth, and resolution of the accelerometers currently available.

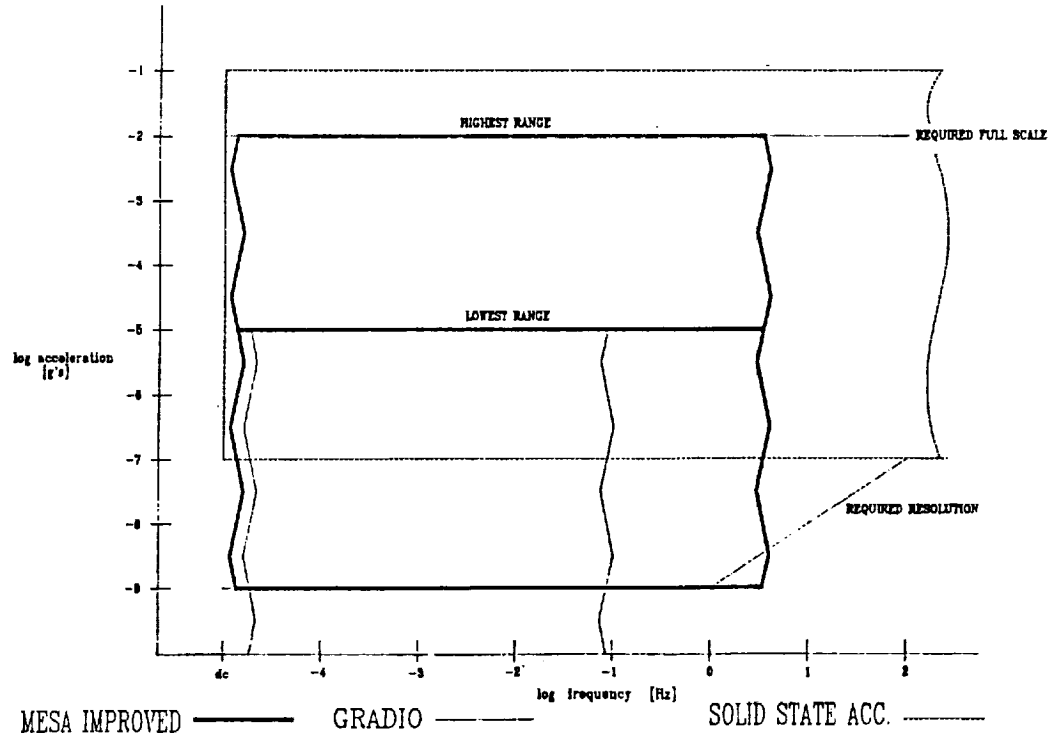

Fig. 5.3 - Full scale, bandwidth, resolution of the accelerometers under development.

5.3 CONCLUSIONS

The principal advantage offered by the VGL is represented by the possibility of exposing the payload to different microgravity values. This represent also the principal difference with respect to the other microgravity missions, in which the experiments are always maintained at the same acceleration level. As a consequence, the monitoring of the microgravity environment on the VGL, as well as the operations of positioning of the elevator itself along the tether, need the measure of accelerations characterized by a wide dynamic range.
By putting together this requirement with those on the measurement accuracy and frequency band, imposed by the scientists, we get a set of characteristics which is very difficult to find within a single sensor.
In fact, in spite of the lack of some information, we can state that no one out of the considered accelerometers, both currently available and under development, is able fulfil all the requirements on range, frequency response, and sensitivity, alone; the same conclusion applies also to the set of sensors including the MESA, the CACTUS, and the Q-flex together. It seems, in fact, very unlikely that the CACTUS and the new version of the MESA have a frequency band from 0 to 100 Hz.
Therefore, if the monitoring requirements listed in the paragraph 5.1 will be considered essential for getting meaningful scientific results, we can conclude that the state-of-the-art accelerometers are not sufficient.
In this case two possibilities could occur:

1) make use of two or more sensors among those under development,

2) start the design and development of new accelerometer(s) tailored on the previously defined requirements.

Again, a definitive answer about the feasibility of the first solution can be given only when complete sets of data about the envisaged performances of the new sensors will be available by the accelerometers manufacturers.

If, instead, we want to make use of the available sensors it is necessary to give up at least one order of magnitude in resolution, and, perhaps, also in bandwidth.
This goal could be achieve, without modifying the nominal mission of the VGL, by reducing, for instance, the measure accuracy required by the scientists down to 50% of the measurement itself (at least for the level 10^{-7} g), and by accepting a value for the sensor resolution only half an order of magnitude below the smallest signal to be mea-

sensitivity can be raised to 10^{-8} g, a value which can be matched by the MESA. If, in addition, in agreement with the scientists, it will be possible to restrict the acceleration monitoring within the frequency band 0-10 Hz, the MESA only could be sufficient for meeting all the requirements (see fig. 5.2); otherwise it will be necessary to make use of the MESA and the temperature-controlled Q-flex together.

Nevertheless the comparison of the full-scale, frequency response, and resolution of the various sensors with those required for the VGL, alone it is not sufficient for giving definitive solution to the problem of the accelerations measurement. To this end other information are needed from the accelerometers manufacturers. In particular a precise knowledge of the of the behaviour of the measurement errors as function of the amplitude of the input signal is essential for selecting an instrument that must detect accelerations with a dynamic range of at least 120 dB.
In view of these further information it will be possible to decide if the whole acceleration range can be covered by a single accelerometer (provided, for instance, with an autorange system), or it will be necessary to have recourse to more sensors (each optimised for a dynamic range of 40 or 60 dB).
Another factor which can drive the choice of the type and the number of instruments is the precise determination in real time of the steady (or near-steady) components of the measured acceleration, required for supporting the positioning operations.
As the accurate detection of the steady-state or slowly varying accelerations within an accelerometer readout containing 10 or 100 Hz - frequency signals is still an unsolved problem, it could be necessary to split also the frequency band in intervals of smaller amplitude, to be covered by different sensors. By using, for instance, an accelerometer sensitive in the frequency regime $0 - 10^{-4}$ Hz, we can get from its output, and therefore in real time, the value of the gravity gradient acceleration inside the VGL, without performing additional analyses.

6. VGL CONFIGURATION HIGHLIGHTS

A summary of the main design decisions and preferred options is thought sensible at this point

6.1 VGL CONFIGURATION CONCEPTS

a) It was decided that the VGL is an elevator; that is it is an object able to move independently along a previously deployed tether.
b) The tether is introduced in the elevator passing through a slot on the elevator itself.
c) The payload is housed in a payload module which is detachable from the VGL itself. The payload module can be an "ad hoc design" which has predetermined mechanical,electrical and electronic interfaces with the elevator.

6.2 VGL SIZE

The VGL mass is estimated to be of the order of 2000 Kg approximately equally divided between payload module and proper elevator.
The typical dimensions of the elevator are of the order of 2 m in height, width and length.

6.3 VGL SUBSYSTEMS

6.3.1 EPDS

The electrical power is supplied mainly by a set of not rechargeable lithium batteries. The batteries mass will be of the order of 300 to 600 Kg. As supplementary and emergency supply source 1 - 2 m^2 of body mounted solar arrays are foreseen.

6.3.2 Thermal control subsystem

The thermal control subsystem is difficult to define without further definition expecially of the payload.
If the payload module is able to handle its thermal control the preferred options are:
a) semi passive system (louvers, shutters, variable capacity heat pipes)
b) active fluid loops
c) passive system.

6.3.3 ACS

The attitude control subsystem is made by:
a) sensors which are four rate gyros periodically updated by a star sensor and a fine sun sensor (or another star

sensor) looking respectively in the out of plane and flight directions.
b) actuators. A yaw wheel is probably required whereas a combination of cold gas jets and dampers should be sufficient to contain pitch and roll errors

6.3.4 Elevator motion actuators

Two groups of three wheels placed at the "top" and "bottom" of the elevator can provide the required actuators performances maintaining a satisfactory degree of access and visibility. Possibly during station keeping phases another mechanism will act as the elevator brake.

APPENDIX B

SMITHSONIAN ASTROPHYSICAL OBSERVATORY

PROGRESS REPORT # 6

Analytical Investigation of Tethered Gravity Laboratory

Aeritalia Contract 8864153

Progress Report #6

For the period 16 May 1989 through 15 August 1989

Principal Investigator

Dr. Enrico C. Lorenzini

Co-Investigators

Dr. Mario Cosmo
Mr. David A. Arnold

September 1989

Prepared for
Aeritalia, Societá Aerospaziale Italiana
Space System Group, Torino, Italy

Smithsonian Institution
Astrophysical Observatory
Cambridge, Massachusetts 02138

The Smithsonian Astrophysical Observatory
is a member of the
Harvard-Smithsonian Center for Astrophysics

SUMMARY

The activity during this reporting period focused on the attitude dynamics of the Variable Gravity Laboratory (VGL).

Specifically the accelerations generated by the VGL rotational dynamics have been thoroughly analyzed during station-keeping as well as crawling maneuvers.

An accurate modelization of the acceleration environment on board VGL can provide valuable information for the subsequent design phases, namely

- Definition of the Attitude and Orbital Control System (AOCS)

- Allocation of volume available for payload accommodation

- Geometrical configuration and mass distribution of VGL

FIGURE CAPTIONS

Figure 1.	Schematic of VGL with attitude reference frames.
Figure 2.	System oscillatory modes vs. the distance between VGL and Space Station.
Figures 3(a)-3(g).	Dynamic response of the VGL for a Station-keeping at 2667 m off the station with attitude dynamics
Figures 4(a)-4(f).	Spectra of the accelerations acting upon two points within VGL for a station keeping at 2667 m off the Station
Figures 5(a)-5(j).	Dynamic response of the VGL for a crawling maneuver from 2667m to 10242 m off the Station with attitude dynamics.
Figures 6(a)-6(j).	Dynamic response of the VGL for a crawling maneuver from 2667 m to 10242 m off the station with in-plane libration/lateral dampers activated and attitude dynamics.

1.0 INTRODUCTION

This is Progress Report #6 submitted by the Smithsonian Astrophysical Observatory (SAO) under Aeritalia Contract 8864153, "Analytical Investigation of Tethered Gravity Laboratory," Dr. Enrico C. Lorenzini, Principal Investigator. This progress report covers the period from 16 May through 15 August 1989.

2.0 TECHNICAL ACTIVITY DURING REPORTING PERIOD AND PROGRAM STATUS

2.1 VGL Attitude Dynamics

The analysis of the accelerations acting on board VGL has been continued. Specifically the VGL attitude dynamics was taken into account. It is well known that the rotational motion will be one of the major sources of noise upon the accelerations acting on board the Space Station, and as it will be shown in the following, the same happens for the VGL. The rotational effects, however, are somewhat mitigated in the VGL case because of the reduced dimensions and distribution of mass.

2.1.1 Mathematical Model

In SAO's MASTER20 code the attitude motion of the Elevator is described with respect to a body reference frame with the origin located in the platform's center of mass and the axis x_1, x_2, x_3 oriented along the three principal axes (Figure 1).

A 3-1-3 rotation sequence has been chosen to define the three Euler's angles with respect to the inertial reference frame[1]. The three Euler's equations can be written as[2]

$$I_1 \dot{\omega}_1 + (I_3-I_2)\ \omega_2 \omega_3 - L_1 = 0$$

$$I_2 \dot{\omega}_2 + (I_1-I_3)\ \omega_1\omega_3 - L_2 = 0 \qquad (1)$$

$$I_3 \dot{\omega}_3 + (I_2 - I_1)\ \omega_1\omega_2 - L_3 = 0$$

where I_1, I_2, and I_3 are the moments of inertia around the principal axes x_1, x_2, and x_3 respectively, ω_1, ω_2, ω_3 are the component of the angular velocity $\underline{\Omega}$, and L_1, L_2, and L_3 are the components of the external torque applied to the VGL. Equations (1) are numerically integrated with the three kinematics equations that relate $\underline{\Omega}$, to the Euler angle rate $\underline{\dot{\alpha}}$ as follows[2]

$$\underline{\dot{\alpha}} = \frac{1}{s\alpha_2} \begin{vmatrix} s\alpha_3 & c\alpha_3 & 0 \\ c\alpha_3 s\alpha_2 & -s\alpha_3 s\alpha_2 & 0 \\ -s\alpha_3 c\alpha_2 & -c\alpha_3 c\alpha_2 & s\alpha_2 \end{vmatrix} \underline{\Omega}$$

where s stands for sine( ) and c stands for cosine ( ).

A better description of VGL's rotational motion is given by erecting a reference frame x_A, y_A, z_A with the origin located at the VGL's center of mass and axes defined as[1]

x_A - axis — along the VGL velocity component in the orbital plane

z_A - axis — along the local vertical toward the Earth

y_A - axis — completes the right-handed reference frame

It is well known that the three rotational displacements of the body reference frame from the x_A, y_A, z_A frame are the yaw angle ψ the pitch angle β and the roll angle γ (3-2-1 rotation sequence).

The external torques are computed by taking only the contributions of the tether tensions into account (elastic and viscous terms). MASTER20, however, can handle also the aerodynamic torques provided that the coordinates of the center of pressure are given as a input.

2.1.2 VGL Attitude Modes

The preliminary VGL geometrical configuration chosen by Aeritalia for the 2000 kg-Elevator is

1.7 m	in-plane flight direction
1.3 m	vertical direction
1.2 m	out-of-plane flight direction

The principal moments of inertia are

$$I_1 = 608 \text{ kg-m}^2$$

$$I_2 = 763 \text{ kg-m}^2$$

$$I_3 = 808 \text{ kg-m}^2$$

The equations which describe the attitude dynamics of the VGL orbiting the Earth at constant rate $\underline{\Omega}$ under the assumption of small angles, are[3]:

$$\begin{aligned} &\text{roll)} && \ddot{\gamma} + a\,\Omega^2\gamma - (1-a)\Omega\dot{\psi} = -(T_1 + T_2)\,\delta\gamma/I_1 \\ &\text{yaw)} && \ddot{\psi} + b\,\Omega^2\psi - (1-b)\,\Omega\,\dot{\gamma} = 0 \\ &\text{pitch)} && \ddot{\beta} + c\,\Omega^2\beta = -(T_1+T_2)\,\delta\beta/I_2 \end{aligned} \qquad (2)$$

where

$$a = (I_2-I_3)/I_1$$

$$b = (I_2-I_1)/I_3$$

$$c = (I_1-I_3)/I_2$$

T_1= lower tether tension

T_2 = upper tether tension
δ = distance between VGL's center of mass and tethers' attachment points

Under the above mentioned hypotheses the pitch dynamics is decoupled by yaw and roll dynamics. On the other hand the yaw and roll dynamics are coupled. Each mode is excited by the other's rate, but this influence is attenuated by the factors (1-a) for the roll and (1-b) for the yaw. In our case, (1-a) and (1-b) are almost equal to unity.

Equations (2) can assume a more compact form if one notes that for our purposes

$$(T_1+T_2)\delta / I_1 >> a\,\Omega^2$$

$$(T_1+T_2)\delta / I_2 >> c\,\Omega^2$$

so that

roll) $$\ddot{\gamma} + \frac{k}{I_1}\gamma = (1-a)\,\Omega\,\dot{\psi}$$

yaw) $$\ddot{\psi} + b\,\Omega^2\,\psi = (1-b)\,\Omega\,\dot{\gamma}$$

pitch) $$\ddot{\beta} + \frac{k}{I_2}\beta = 0$$

where $k = (T_1+T_2)\delta$

The pitch natural frequency f_p is

$$f_p = \frac{1}{2\pi}\sqrt{\frac{k}{I_2}}$$

Figure 2 shows the pitch frequency for our system and the lateral and longitudinal frequencies versus the distance of the VGL from the Space Station. The pitch frequency is comprised between the two spring-mass modes' frequencies and ranges from 7.1×10^{-2} Hz with VGL at the orbital center to 8.2×10^{-2} with VGL at 10242 m off the Space Station (4×10^{-3} g location). No resonance appears even though

the analysis should be completed to include the tethers' higher modes (longitudinal and lateral).

2.1.3 Rotational Acceleration Noise on Board VGL

The acceleration measured by an accelerometer package in a point P shifted from the VGL's Center of Mass with the sensors aligned with the body axes can be expressed as

$$\underline{A}_P \simeq - [\underline{A}_{CM} + \dot{\underline{\Omega}} \times \underline{r}_P + \underline{\Omega} \times (\underline{\Omega} \times \underline{r}_P)] \qquad (4)$$

where

$\underline{r}_P$ = position vector of P with respect to the body reference frame

$\underline{\Omega}$ = angular rate of the body reference frame

A_{CM} = acceleration at the VGL's Center of Mass

The minus sign indicates that the acceleration A_p is apparent and therefore opposed to the inertial. The ~ sign means that the gravity gradient acceleration due to the shift, at most equal to 2.5×10^{-7} g, has been neglected.

From the right-hand side of equation (4) it is evident how the tangential (2nd) and the centrifugal terms (3rd) can limit the volume where the low-gravity experiments are carried out. In fact, even though the geometrical dimensions of the VGL are small, large angular rates or their derivatives can reduce the space available for experiments. All this however has to be assessed quantitatively in order to provide adequate damping techniques.

2.2 Numerical Simulations

Numerical simulations have been run to show how the attitude motion affects the acceleration field on board VGL, namely:

A) Station keeping with VGL at 2667 m off the Space Station

B) VGL crawling from 2667 m to 10242 m off the Space Station

C) Same as B) but with the in-plane libration/lateral dampers activated

Note that the crawling maneuvers as well as run A) have been already shown in Progress Reports # 4 and 5. Our purpose is just to relate the system dynamics with the VGL's rotational motion.

2.2.1 VGL Dynamics Response for Station-Keeping

Figures 3(a)-3(g) show the dynamic response of run A). Comparing the in-plane angle θ and out-of-plane angle ϕ [Figure 3(a)] with the pitch and roll angles respectively [Figure 3(b) and 3(c)], we note that they have similar behavior. The low-frequency librations of the system are driving the whole dynamics. A higher frequency component, however, is superimposed on the pitch and roll modes due to their natural frequencies. The yaw angle shown in Figure 3(d) is influenced by the roll rate according to equations (3), but the amplitude of oscillation is smaller than the roll's. Figures 3(e), 3(f), and 3(g) show the acceleration components acting on VGL's center of mass along the body axes. The influence of the VGL rotation is particularly evident for the component acting along axis 1. Note, however, that this is not what we refer as "rotational noise" [see Equation (4)] but simply a modulation of the accelerations acting on VGL's CM at the attitude's natural frequencies, which are the oscillation modes of the body reference frame.

In order to clarify this concept the data of run (A) have been post-processed using equations (4) to compute the accelerations acting upon other points within VGL's volume, namely

P = P(0.85,0,0) the farthest point on axis 1 (flight direction)

and

Q = Q(0,0,0.65) the lowest point on axis 3 (toward earth)

The spectra of the acceleration components are shown in Figures 4(a)-4(f). Note that the DC component has been subtracted and only the accelerations along axis 1 and 3 have been considered.

With reference to Figure 2, the system's natural frequencies when VGL is at 2667 m off the Station are

I "Spring-mass" mode	1.15×10^{-1} Hz
II "Spring-mass" mode	3.12×10^{-2} Hz
"String-like" mode	9.11×10^{-4} Hz
Pitch mode	7.36×10^{-2} Hz

Due to the complexity of the coupling among the three rotational DOF's it is hard to separate the effects of different contributions on the accelerations components. Nevertheless, the accelerations components along axis 1 [Figures 4(a)-4(c)] seem to be influenced mainly by the "string-like" mode and the pitch mode. The latter mode, actually, plays a major role in the spectra of the acceleration in Q with a peak amplitude of 1.41×10^{-5} g. The opposite happens to the acceleration components along axis-3 [Figures h(d)-h(f)]. Point P, in fact, is the most affected by the pitch mode with a peak amplitude of 1.78×10^{-5} g. This is caused by the action of the tangential term [$\dot{\Omega} \times r$] of the acceleration. Note also in Figure 4(b) a small peak at twice the pitch frequency due to the action of the centrifugal term [$\Omega \times (\Omega \times r)$]. Further studies, however, are needed to understand the complicate coupling of the rotational DOF's.

2.2.2 VGL Dynamic Response for Crawling Maneuvers

The VLG crawling maneuver from 2667 m to 10242 m off the Space Station has been used as test case to study the attitude dynamics of our system when the Elevator is in motion. Note that this case has been already analyzed from different points of view in Progress Report #4.

Main Purposes for studying this case are:

1) To compare the effects of the System's attitude dynamics when the libration/lateral damper is activated or not

2) To assess the presence of undesired build-up of attitude oscillations caused by the Elevator's motion.

As it was pointed out in the previous paragraph, the system's librations are superimposed to the roll and pitch angles so that the activation of the libration/lateral dampers to control the attitude dynamics might be helpful. The libration/lateral damper, however, cannot be considered the solution for damping the rotational modes since it operates in a range of frequencies (~ 10^{-4} Hz) different from the pitch natural frequencies (~7 x 10^{-2} Hz). Only adequate dampers turned on those frequencies can serve the purpose. Figures 5(a)-5(j) show the dynamic response of run B). Figures 5(a) and 5(b) were already shown in Progress Report #4 but are included for the sake of clarity. As it was shown in the previous run, also in this case the system librations θ, and ϕ drive the VGL attitude dynamics [Figure 5(c), 5(d)]. Nevertheless the lateral oscillations are the source which mostly affect the pitch angle when the system has reached the final length. The roll and the yaw angles, instead, show the same feature of run A) [Figure 5(d), 5(e)]. For sake of completeness also the torques acting on axis-1 and axis-2 are shown [Figures 5(f), 5(g)]. Obviously the torque component acting on axis-3 is null. Figures 5(h), 5(i) and 5(j) show the acceleration components acting on board VGL along the three body axes respectively. The attitude frequencies are evident for

the axis-2 component (high frequencies harmonics). On the contrary, because of the lateral dynamics for axis-1 component and of the final dc value for axis-3 component, the attitude frequencies are not visible. This is overcome by activating the in-plane libration/lateral dampers. Figures 6(a)-6(j) show the result of run C).These plots must be compared to the corresponding plots of Figures 5. Note that the run is longer because the crawling starts a little later than run B) in order to activate the dampers without discontinuities. By dissipating the system oscillations (in plane libration and lateral displacement) the dampers decrease the energy transfer to the rotational DOF's. Consequently, the peak-to-peak amplitude of the pitch angle at the end of the maneuver decreases from 1.15 deg [Figure 5(c)] to 10^{-1} deg [Figure 6(c)]. The roll and yaw angles remain unchanged [Figures 6(d) and 6(e)]. The effect of the energy dissipation appears also in the axis-1 acceleration component where only the high frequency harmonic of the pitch mode are present [Figure 6(h)]. The axis-2 component is practically unchanged [Figure 6(i)]. In the case of axis-3 the ripples of the lateral displacement have disappeared but, because of the final dc value, the attitude harmonics are still not visible.

2.3 Conclusion

The analysis of the VGL attitude dynamics has shown that the rotational motion can be source of significant acceleration noise acting upon the laboratory. Severe limits can be posed on the payloads accommodation unless suitable dampers are adopted. The in-plane libration/lateral dampers have shown their effectiveness in limiting the energy transfer from low frequency disturbances but cannot be considered effective attitude dampers since they are not tuned to the attitude frequencies. The analysis will be continued in order to gain better understanding of the VGL attitude dynamics.

2.4 REFERENCES

1. Vetrella, S., A. Moccia, E.C. Lorenzini, and M. Cosmo,"Attitude Dynamics of the Tether Elevator/Crawler System for Micro-Gravity Applications." Proceedings of the 2nd International Conference on Tethers in Space, San Francisco, CA, May 17-19, 1989, pp.323-330.

2. Wertz, J.R. (Ed.), "Spacecraft Attitude Determination and Control," D. Reidel Publishing Company, 1978.

3. Lemke, L.G., J.D. Powell, and X. He, "Attitude Control of a Tethered Spacecraft." The Journal of the Astronautical Sciences, Vol. 35, January-March, 1987, pp. 41-55.

3.0 Problems Encountered During Reporting Period

None.

4.0 Activity Planned for Next Reporting Period

During the next reporting period the analysis of VGL attitude dynamics will be continued. A plan for future studies will be decided at the meeting scheduled in Torino for the end of September.

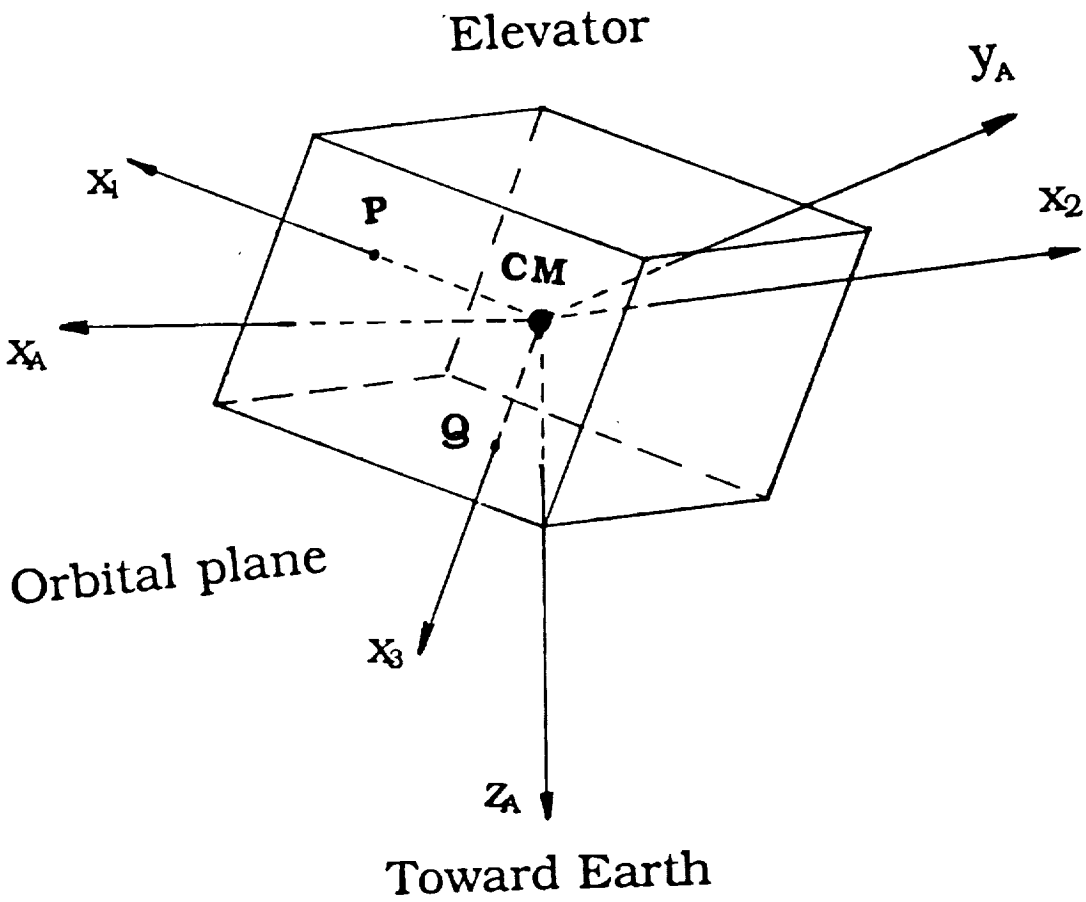

Figure 1.

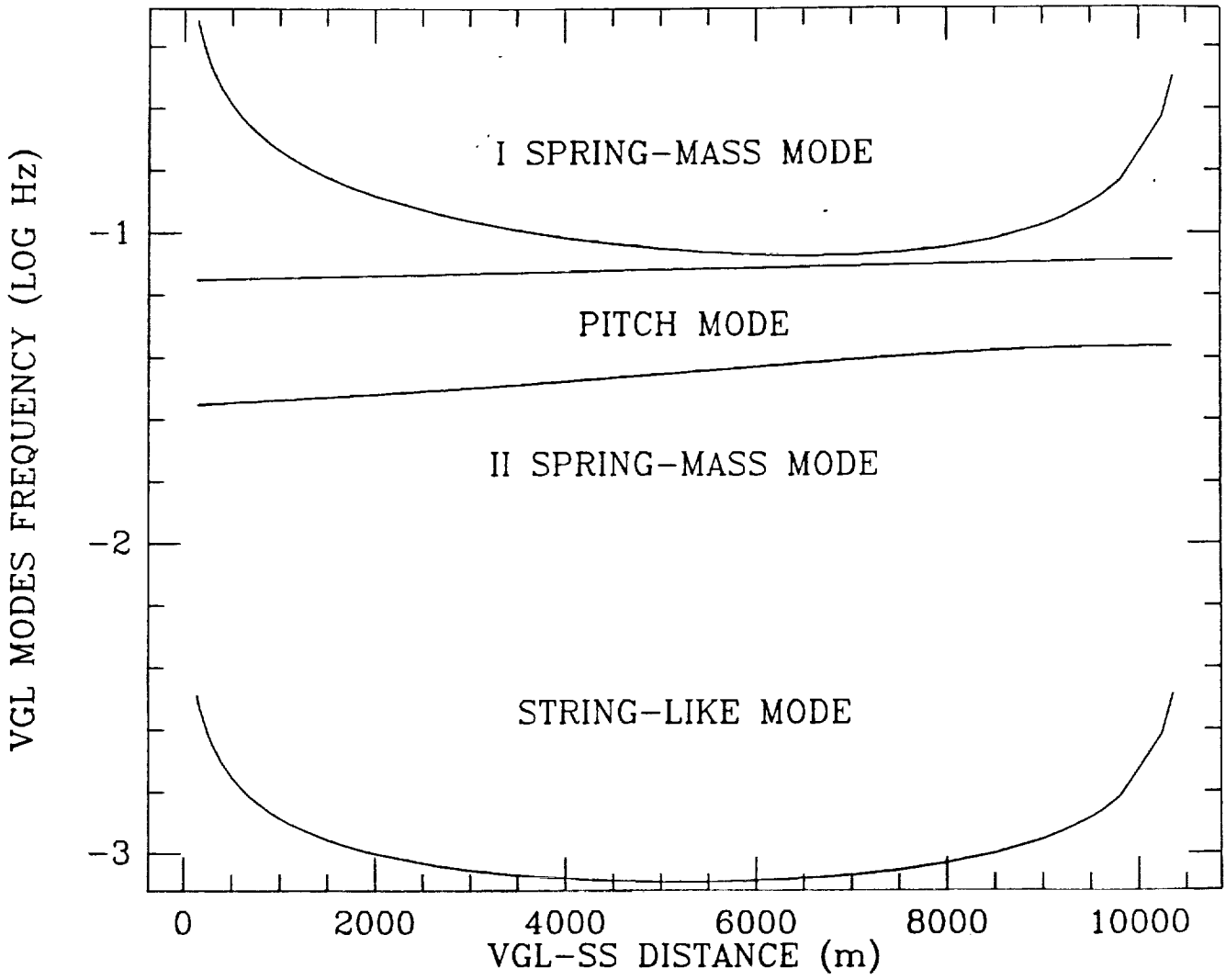
I SPRING-MASS MODE
PITCH MODE
II SPRING-MASS MODE
STRING-LIKE MODE
VGL MODES FREQUENCY (LOG Hz)
-1
-2
-3
0
2000
4000
6000
8000
10000
VGL-SS DISTANCE (m)

Figure 2.

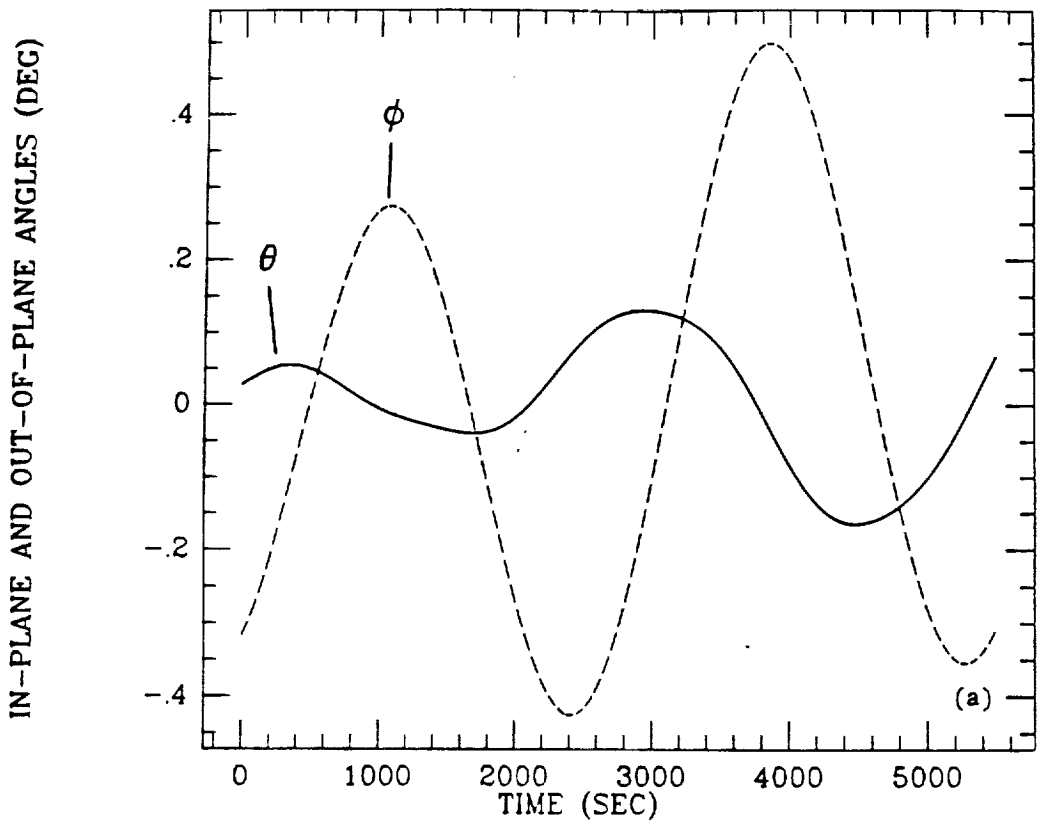

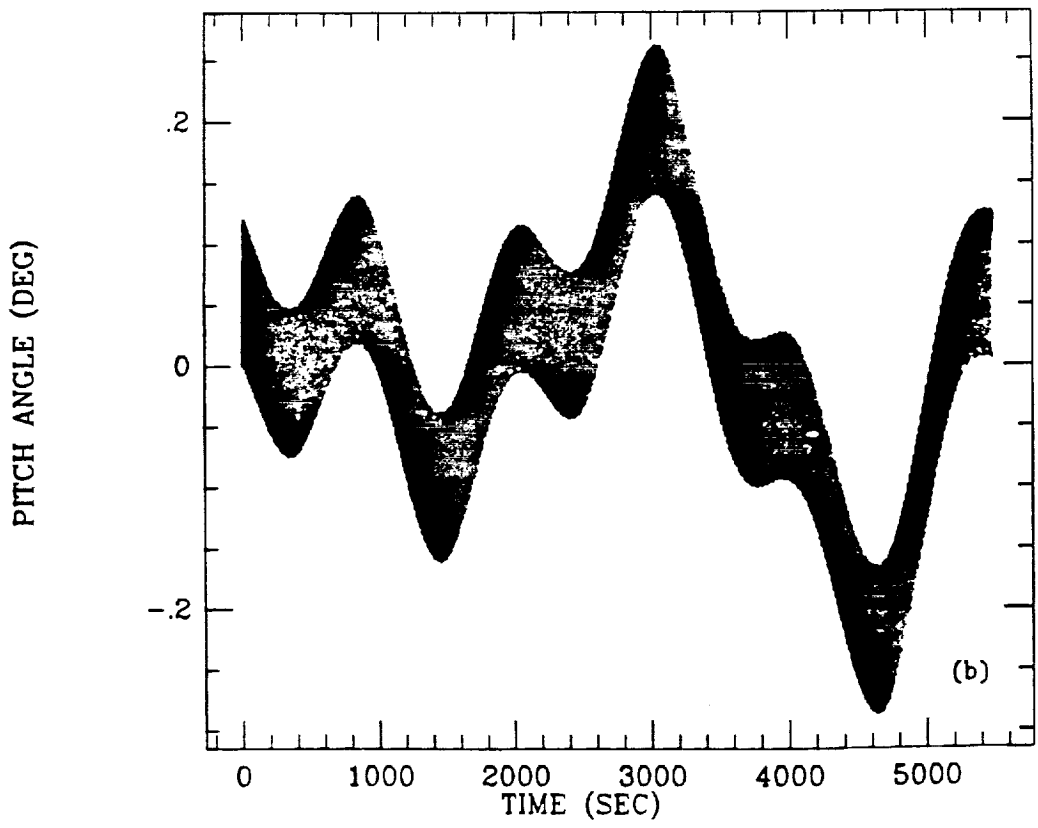

Figures 3(a) and 3(b).

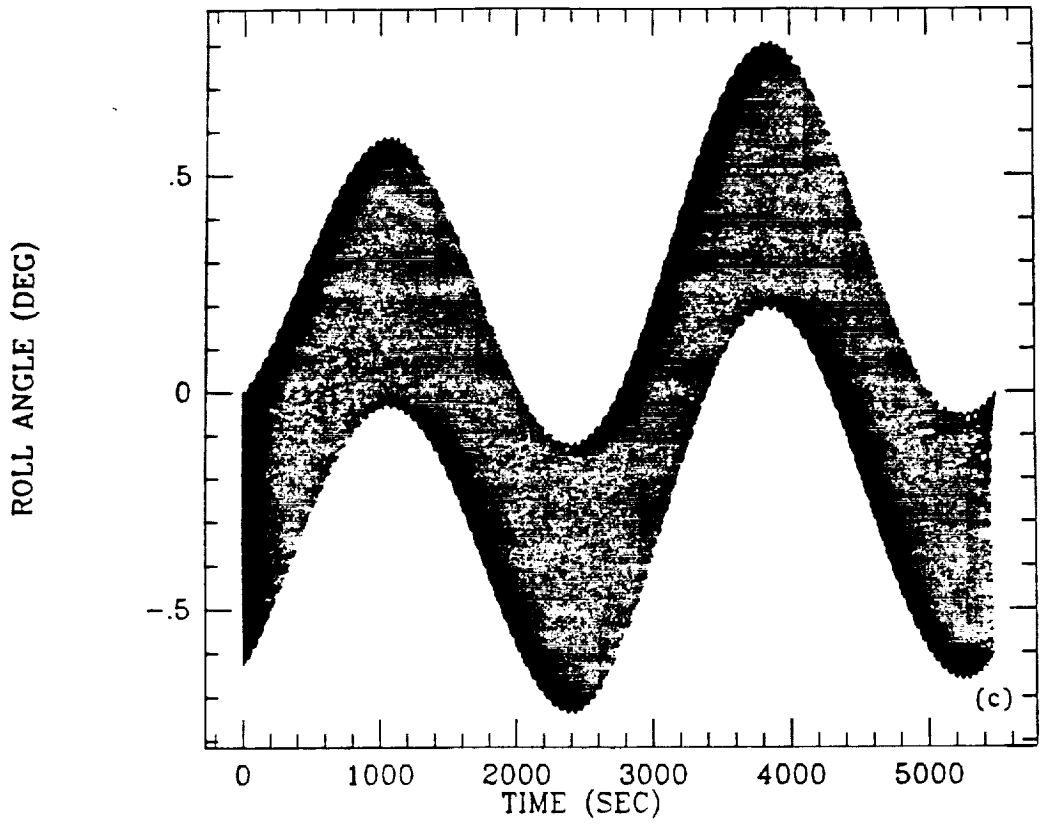

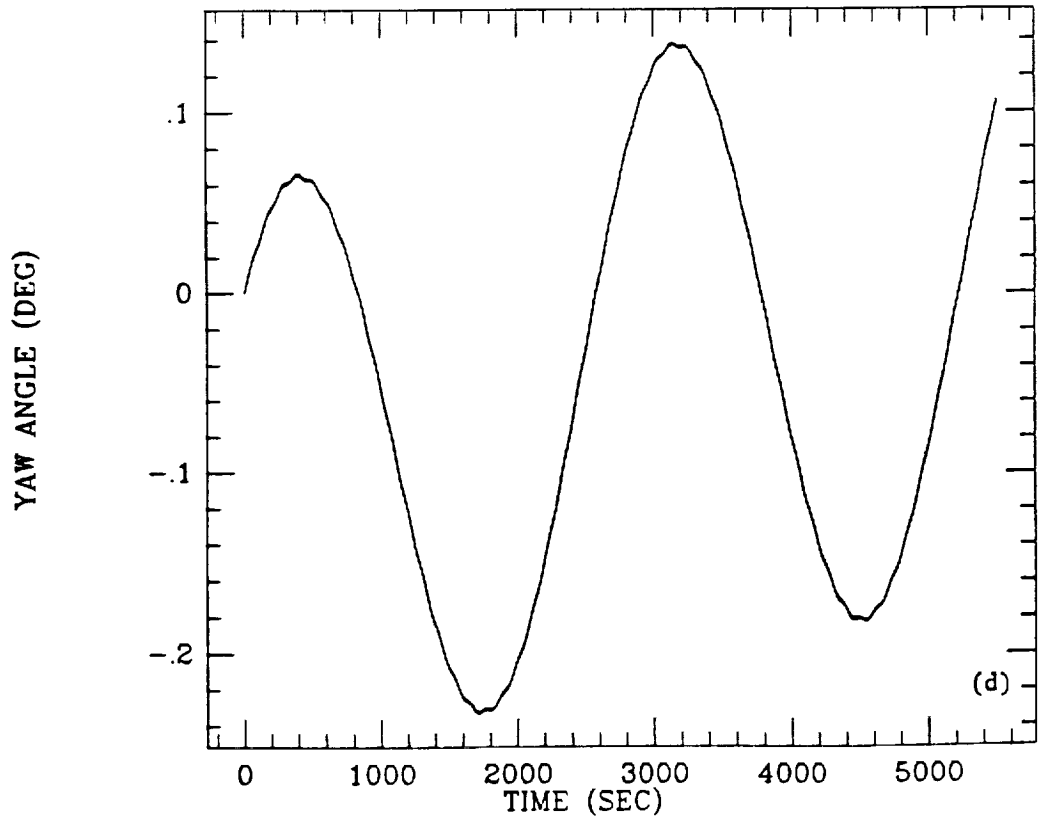

Figures 3(c) and 3(d).

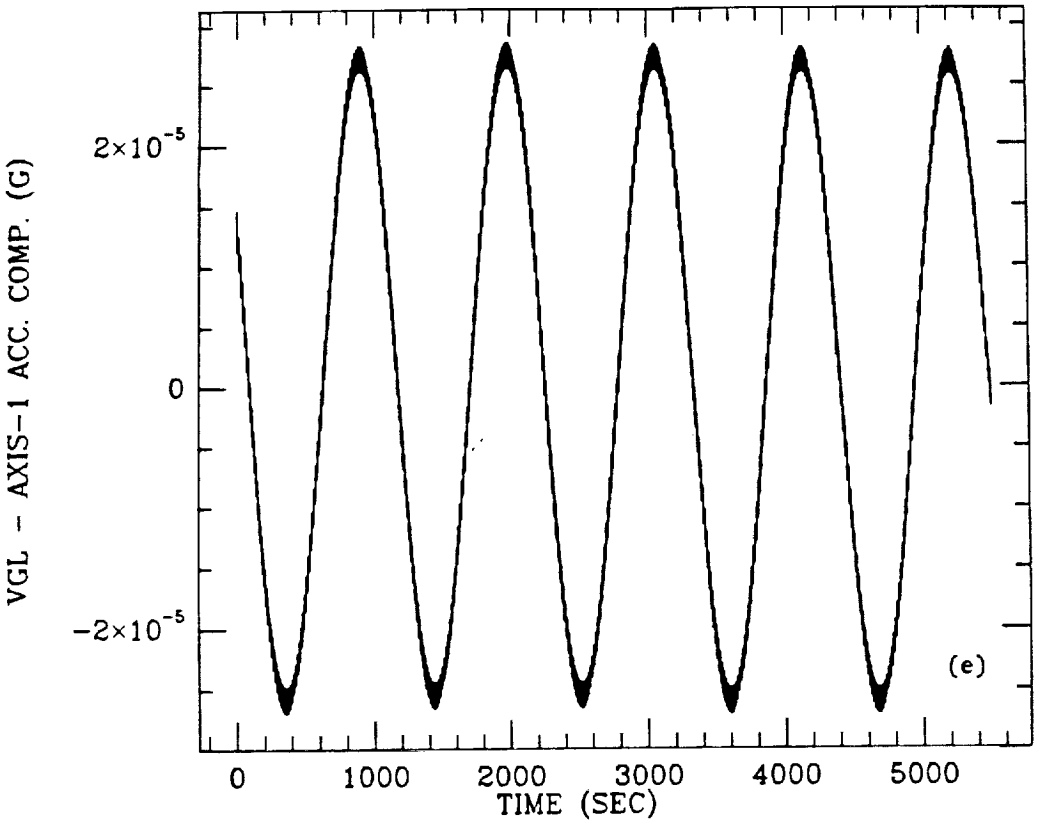

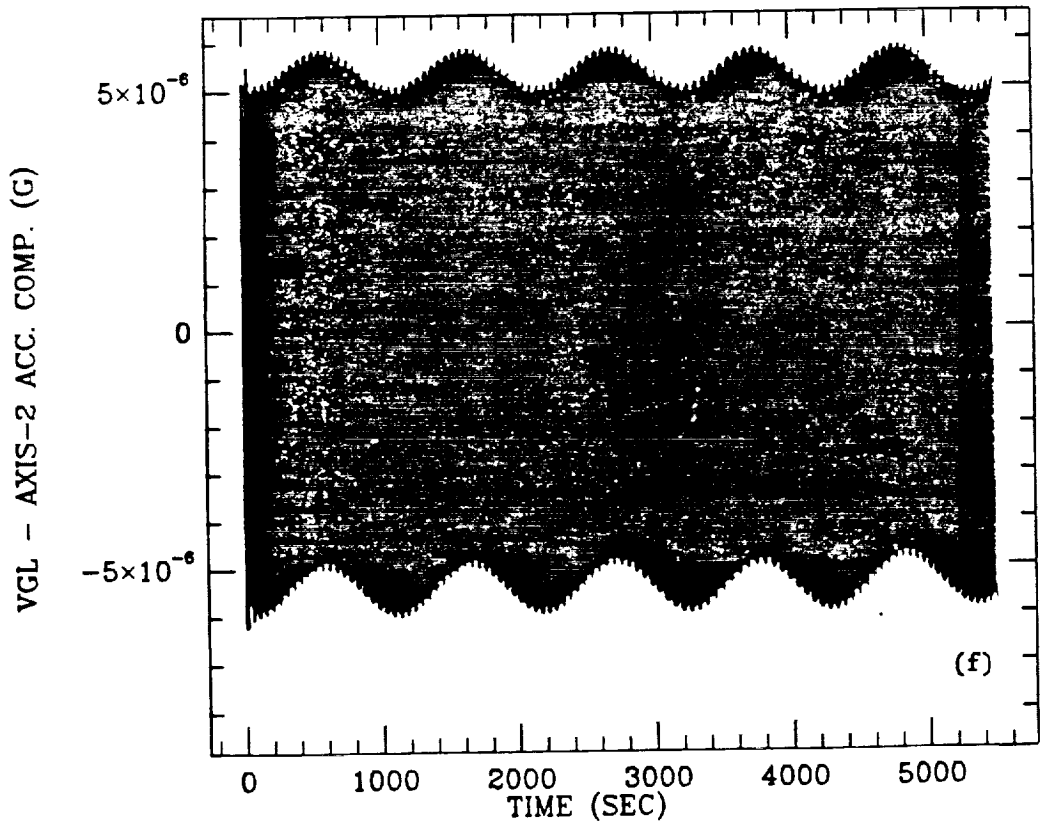

Figures 3(e) and 3(f).

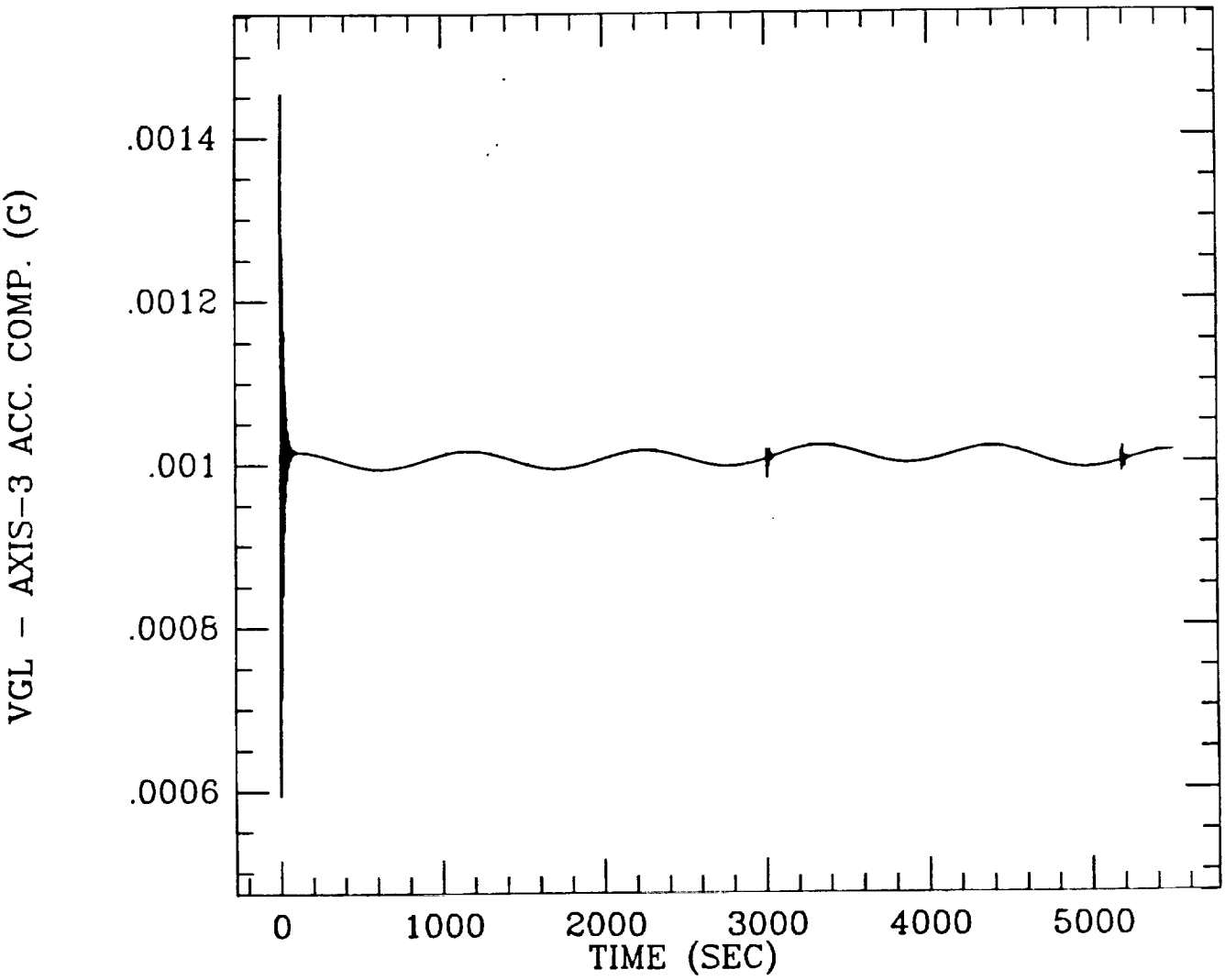
VGL - AXIS-3 ACC. COMP. (G)
.0014
.0012
.001
.0008
.0006
0
1000
2000
3000
4000
5000
TIME (SEC)

Figure 3(g).

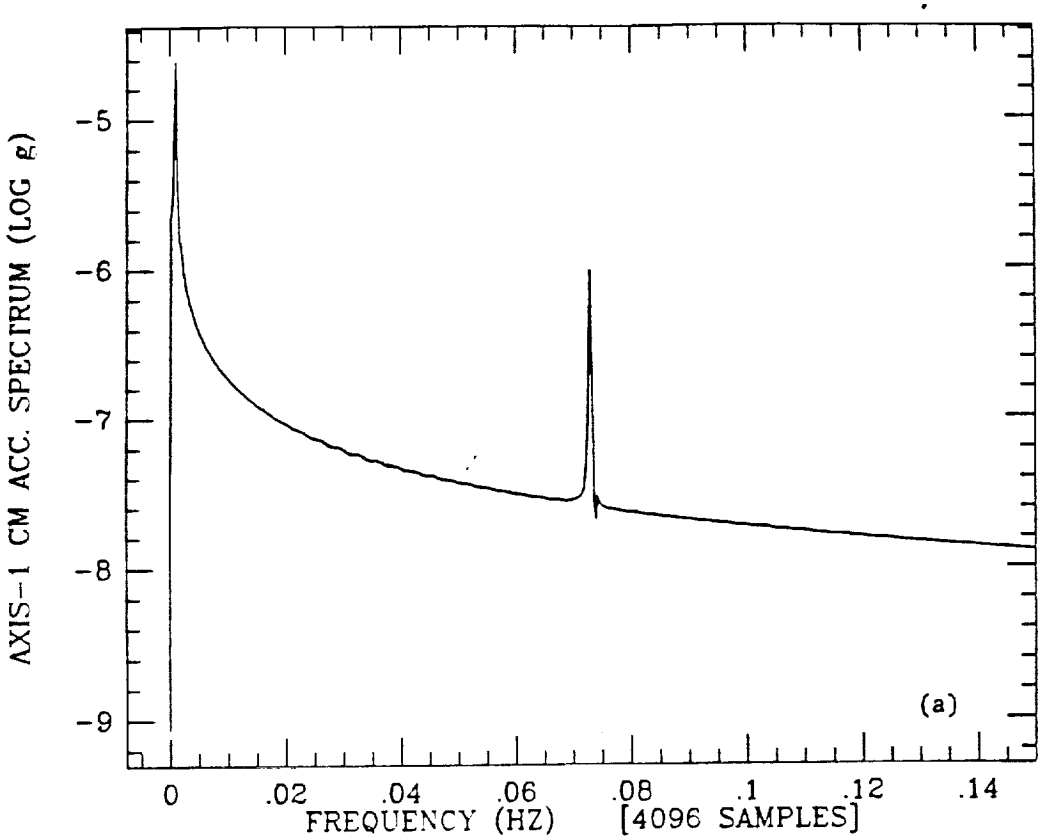

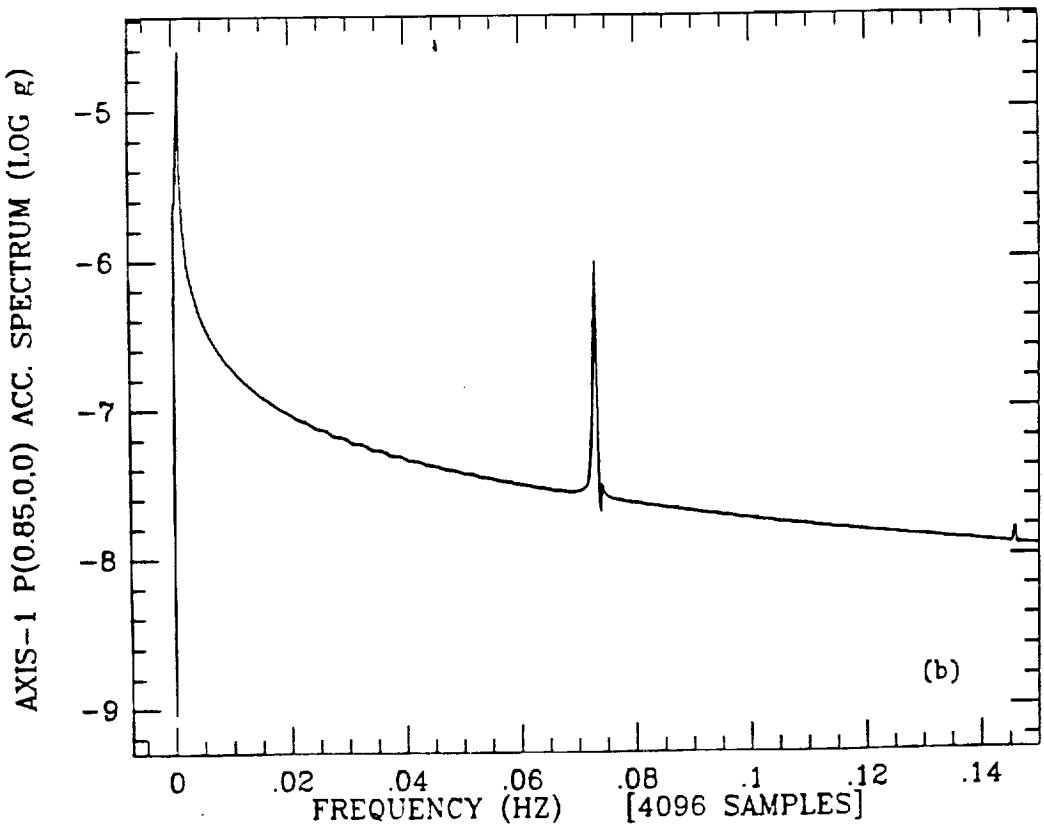

Figures 4(a) and 4(b).

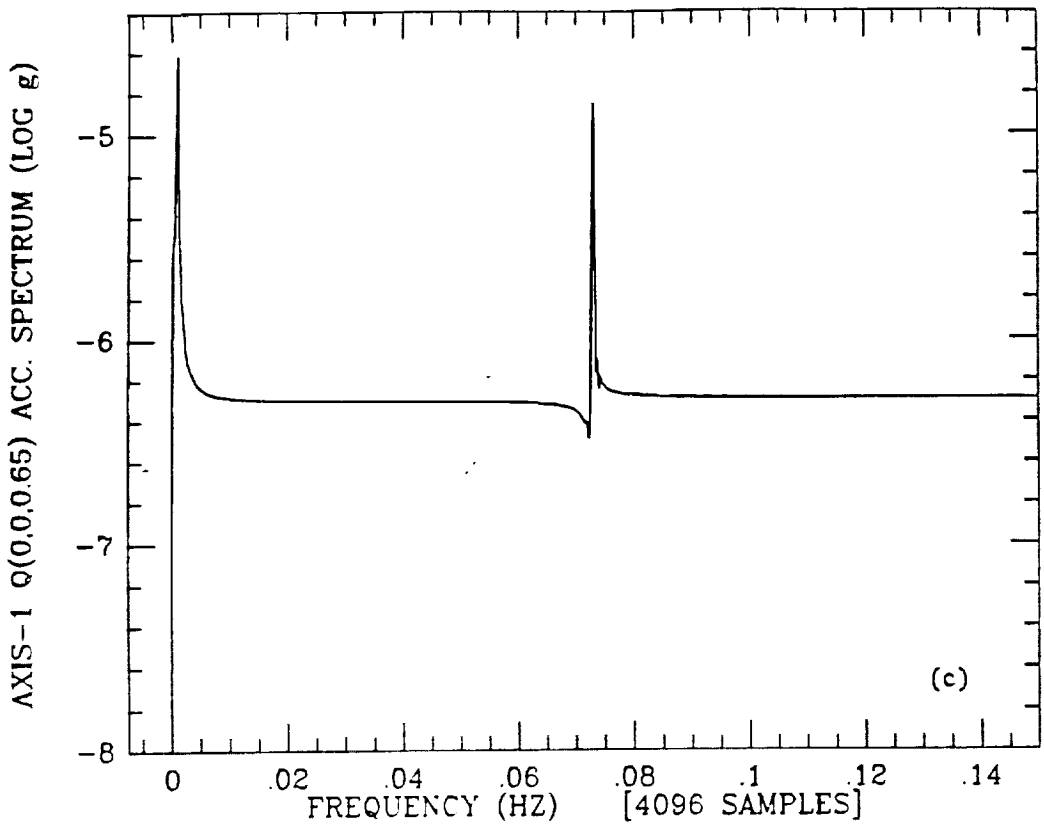

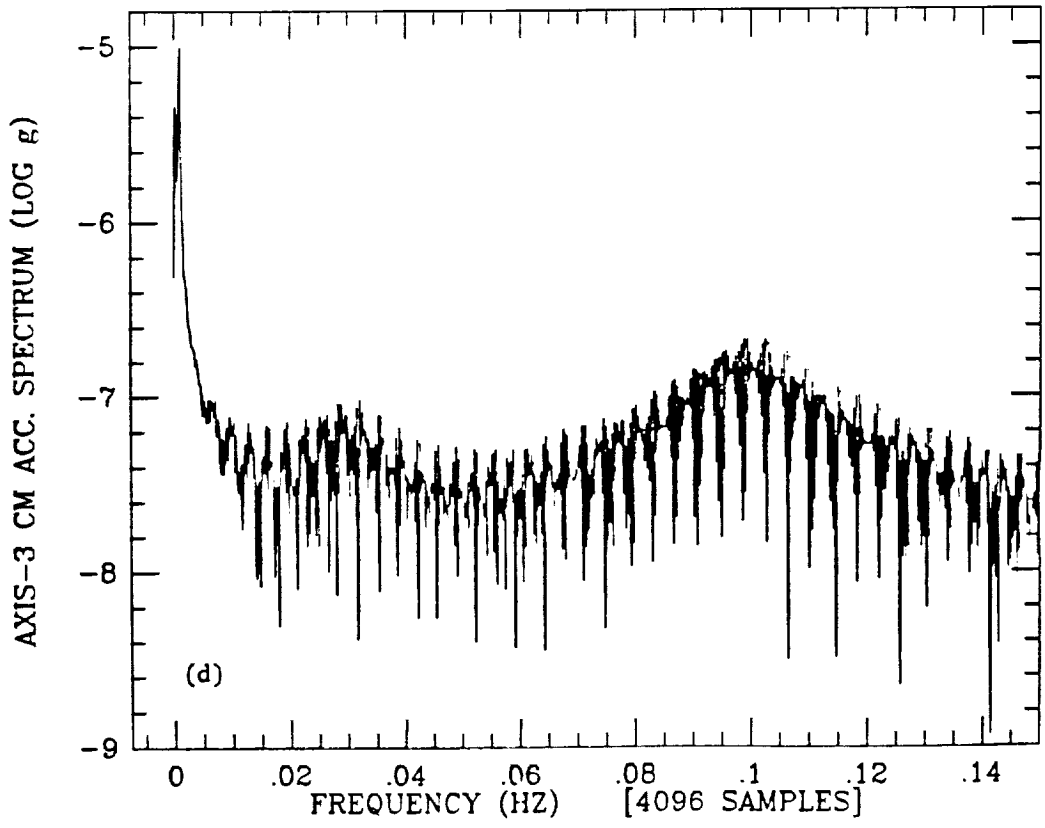

Figures 4(c) and 4(d).

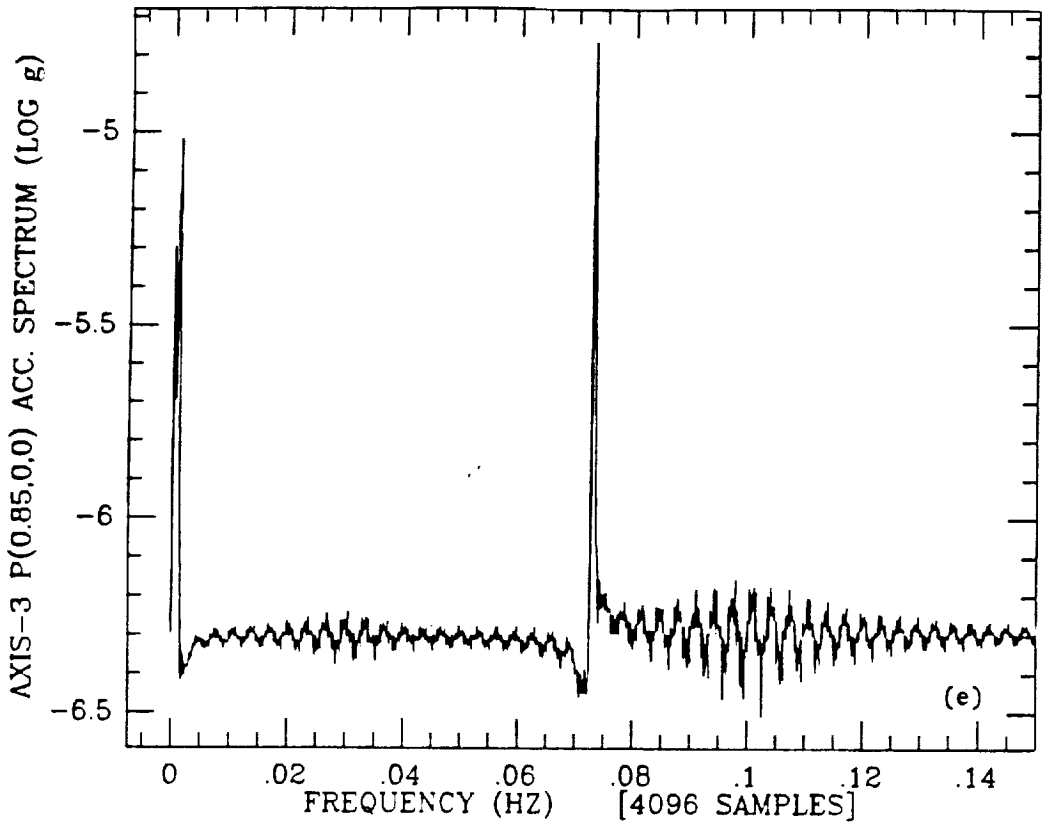

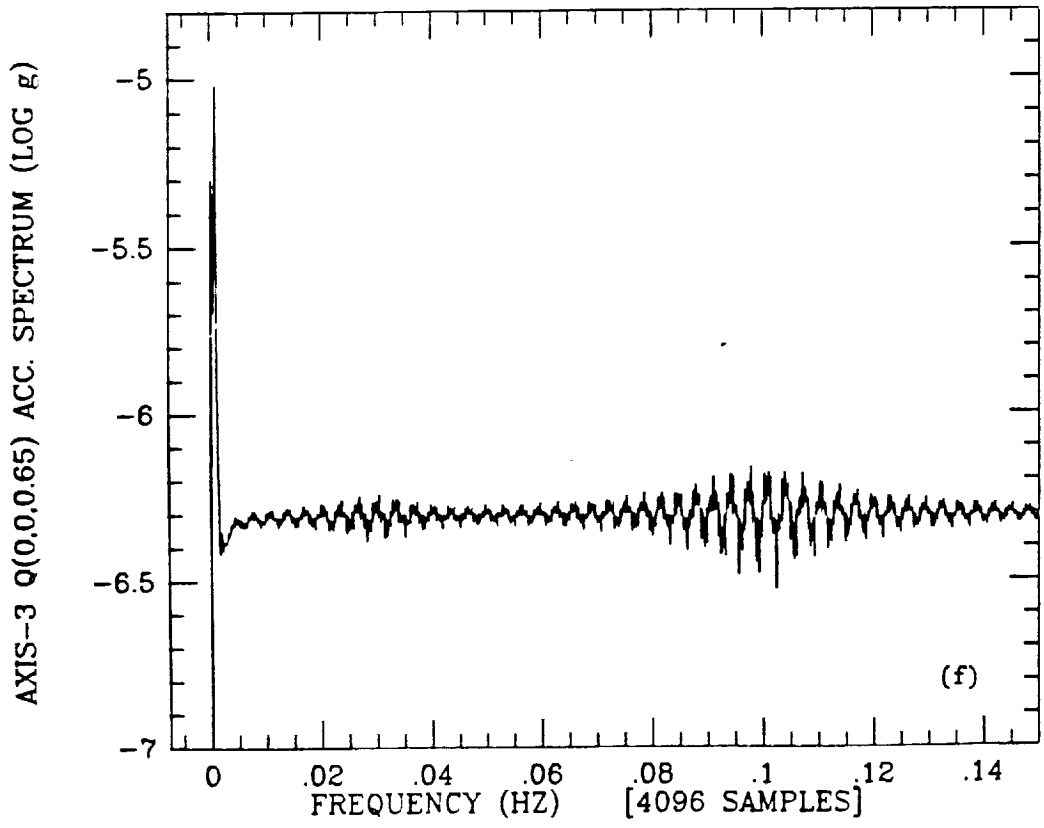

Figures 4(e) and 4(f).

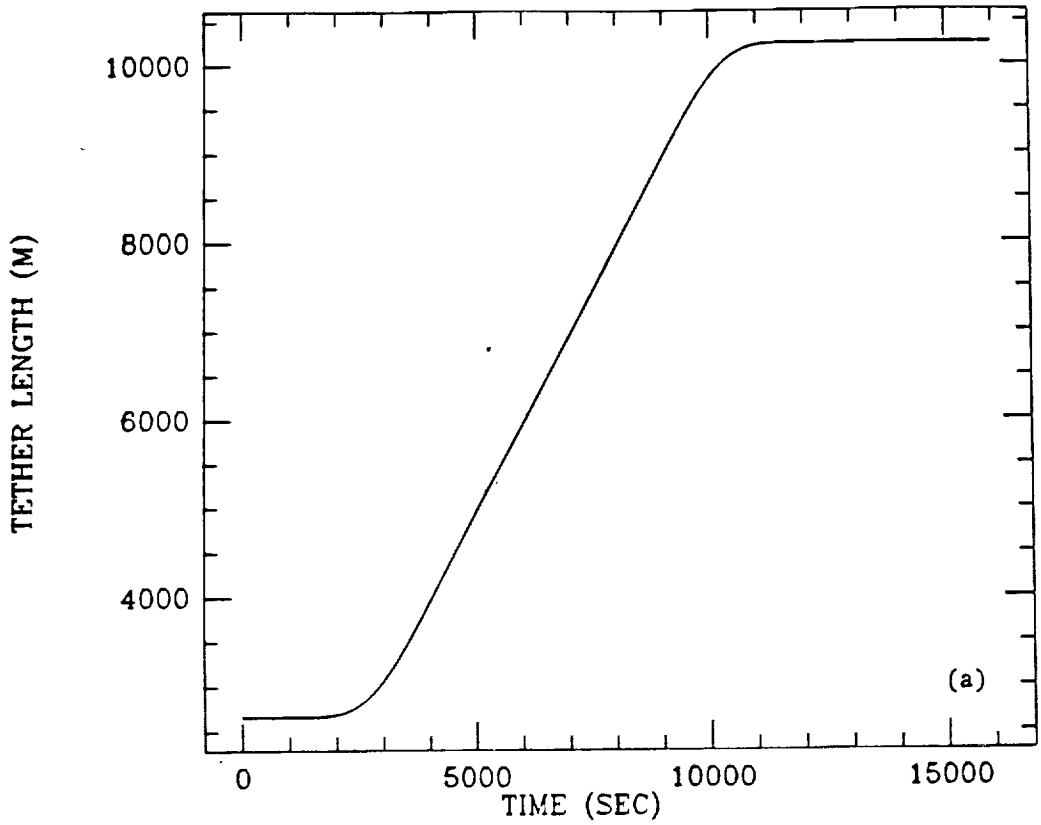

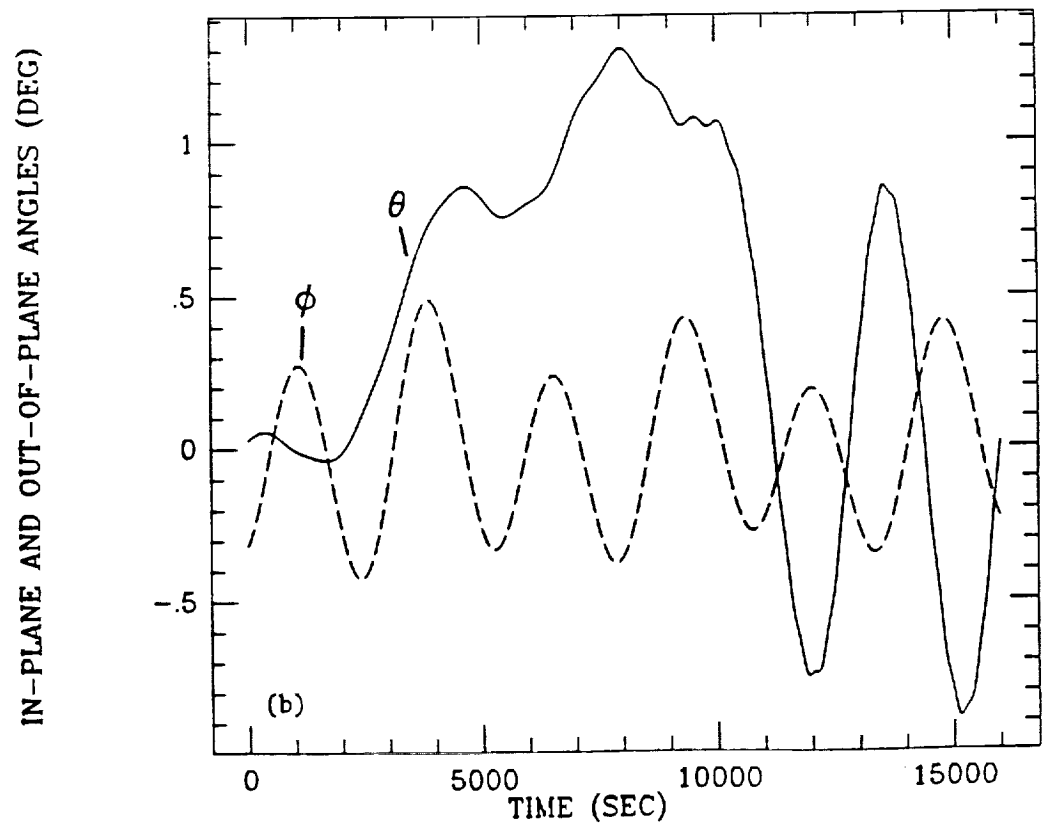

Figures 5(a) and 5(b).

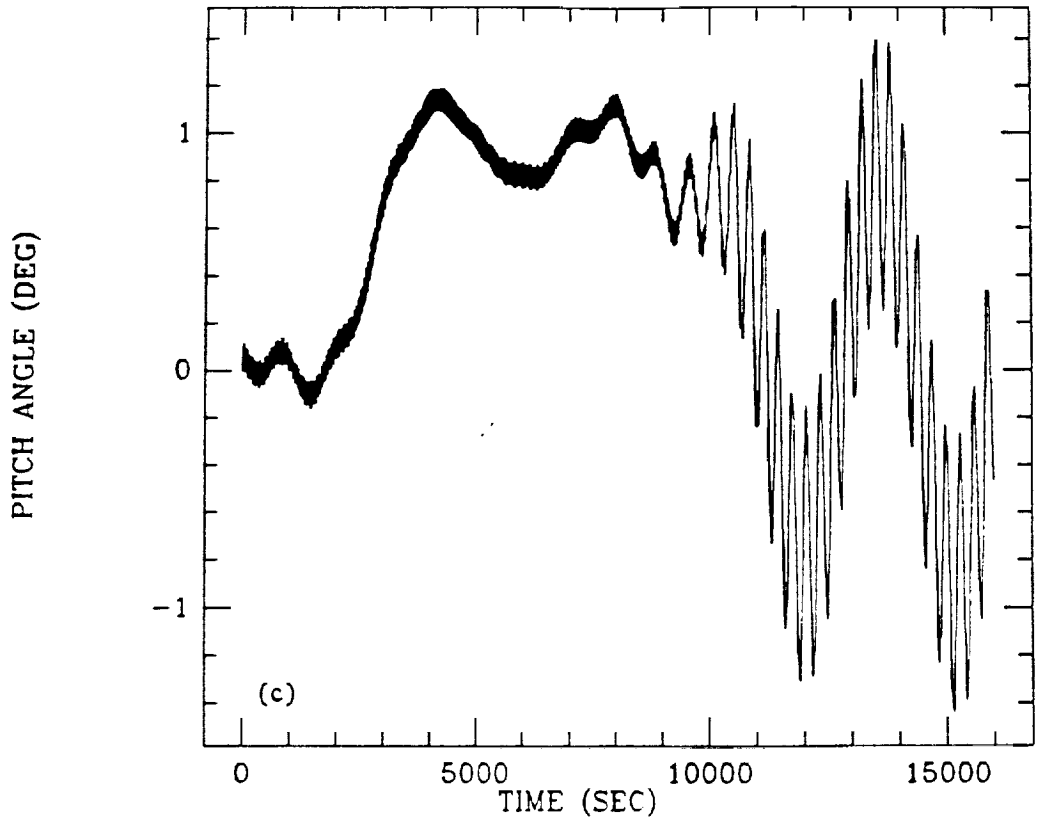

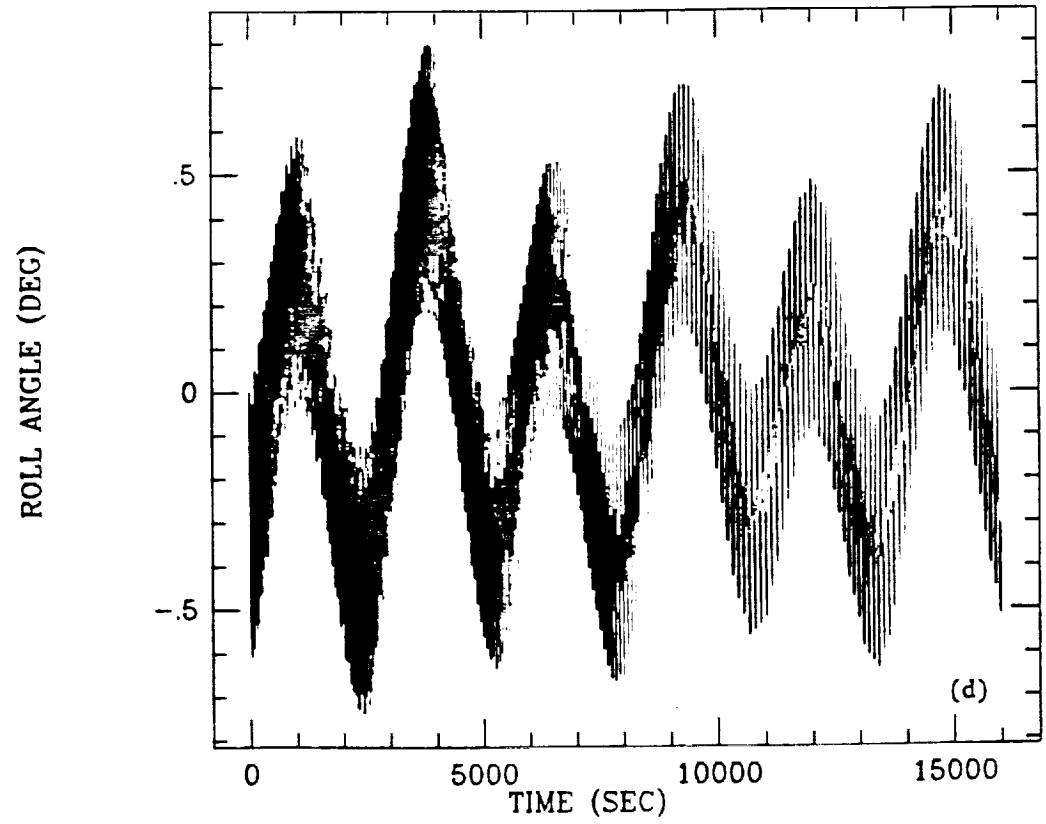

Figures 5(c) and 5(d).

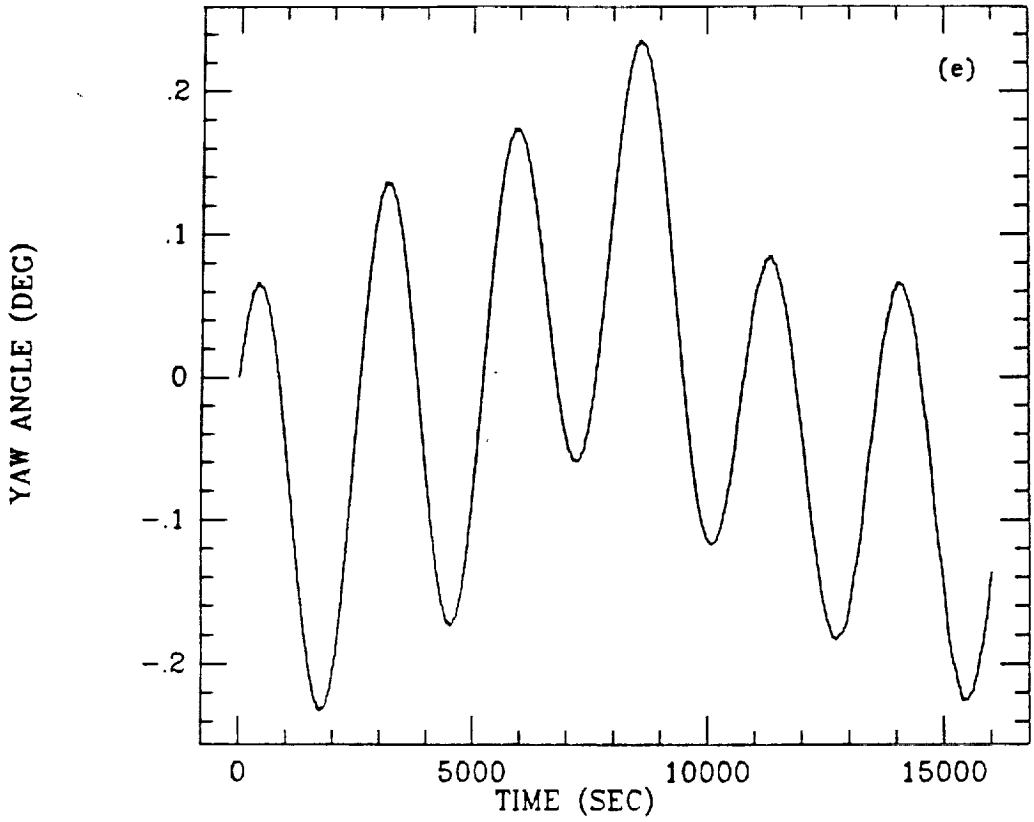

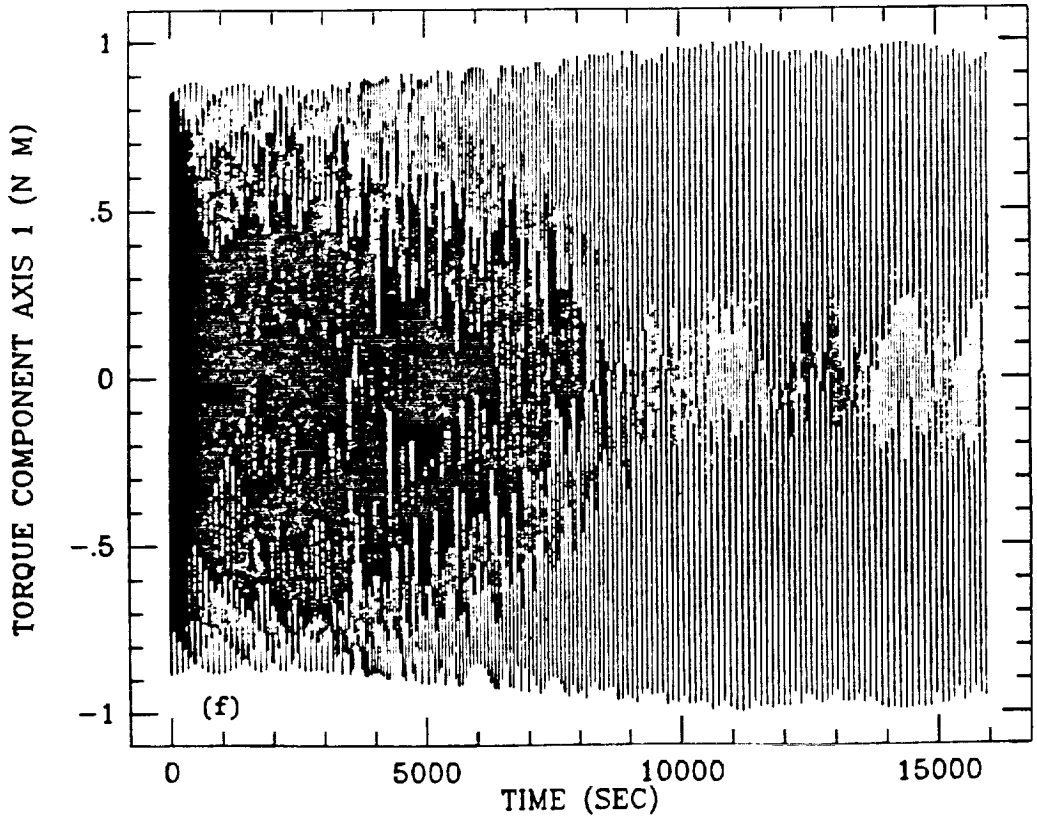

Figures 5(e) and 5(f).

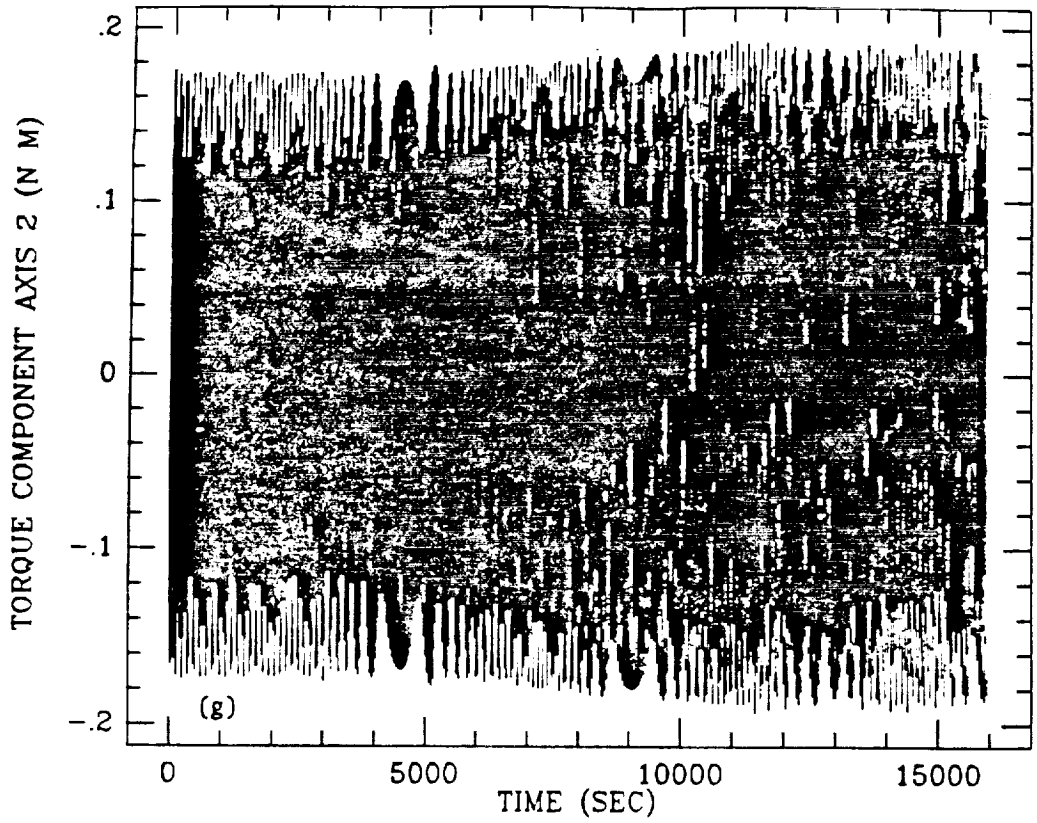

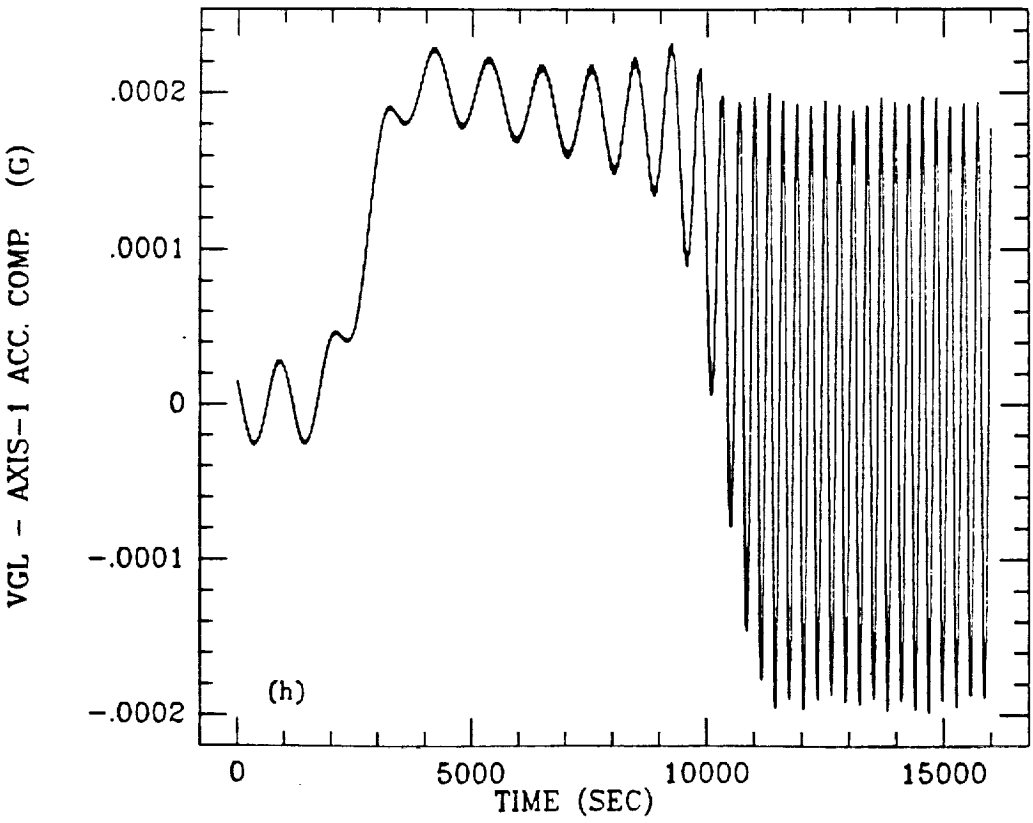

Figures 5(g) and 5(h).

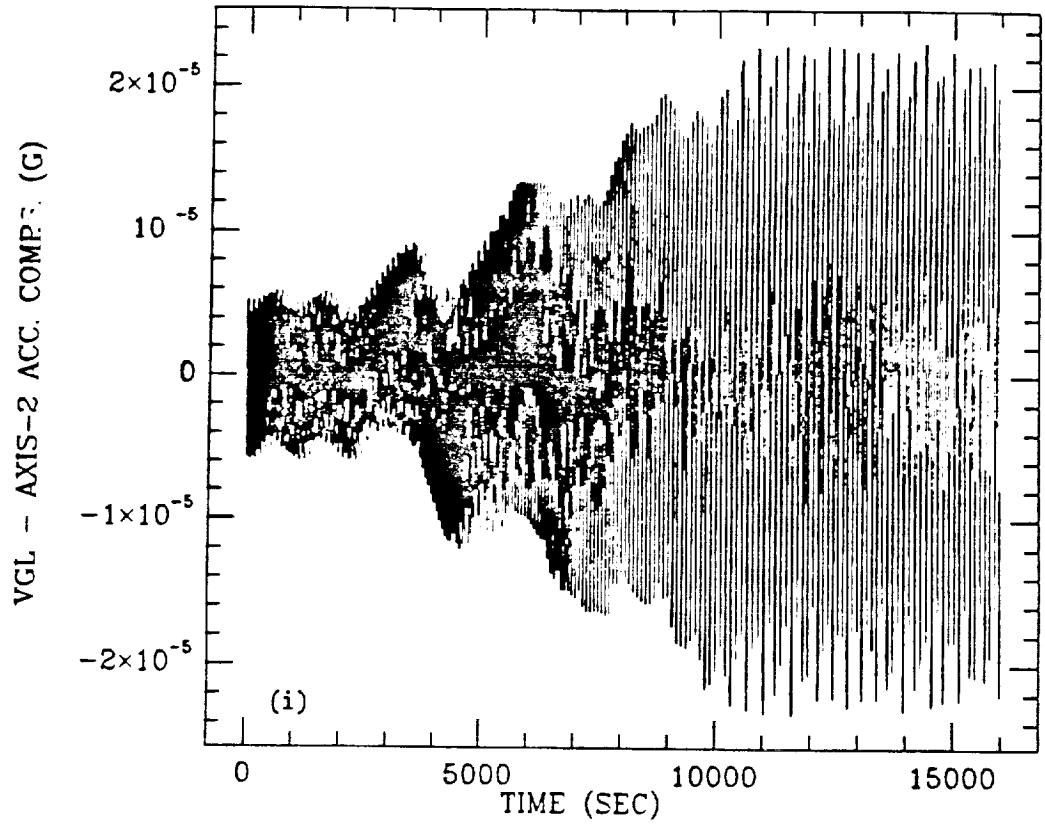

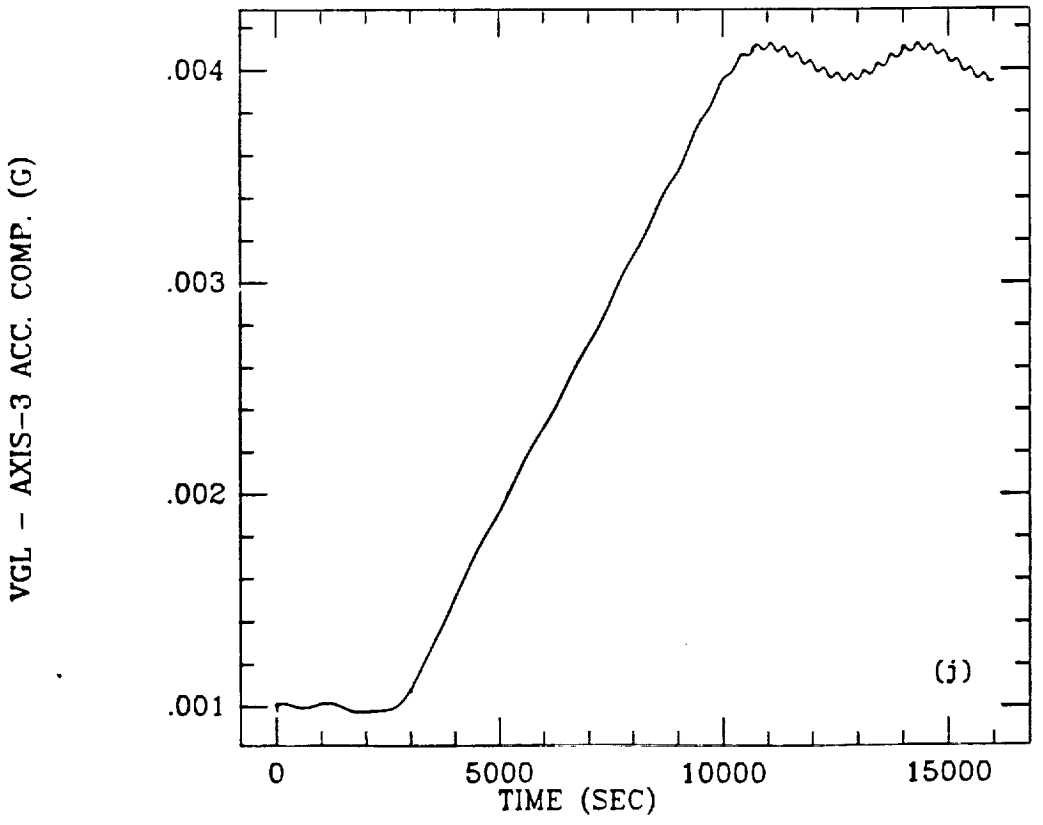

Figures 5(i) and 5(j).

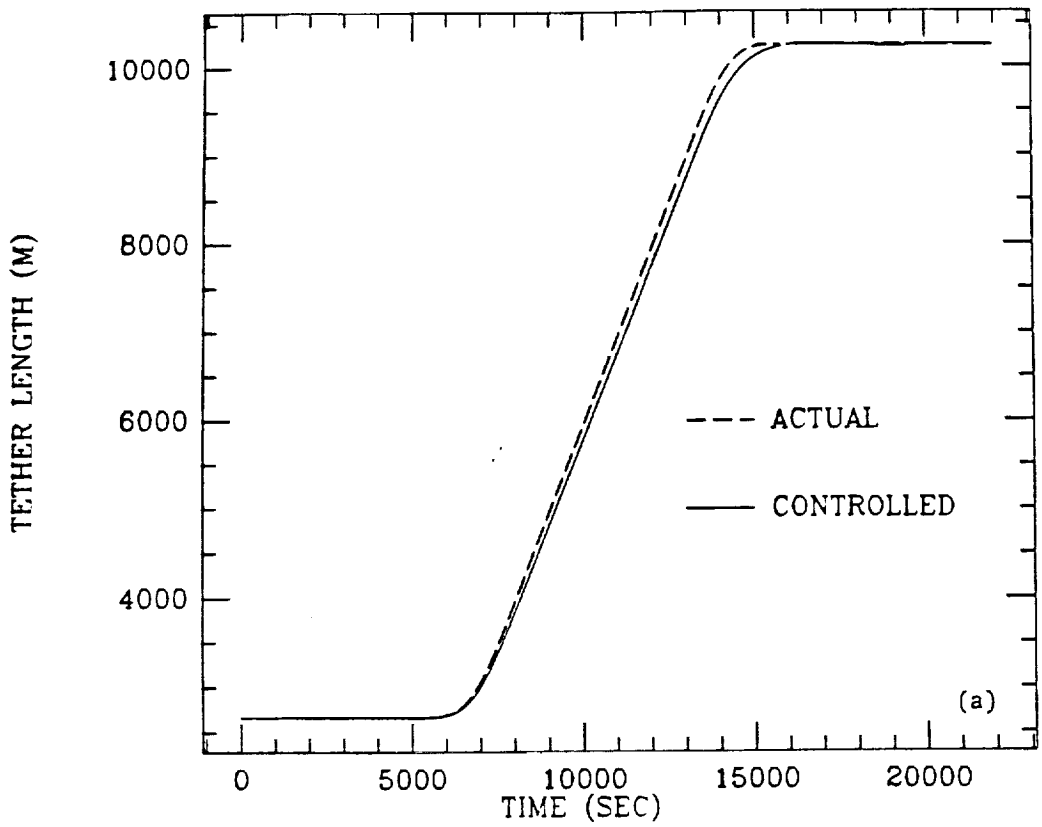

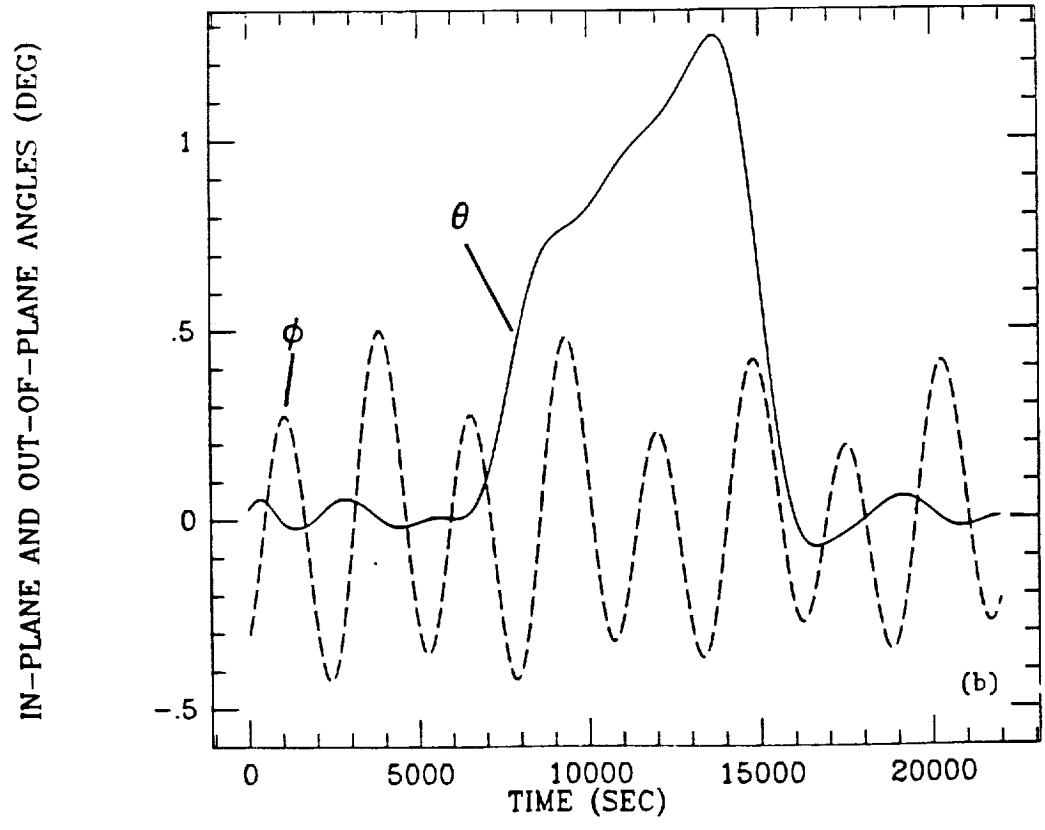

Figures 6(a) and 6(b).

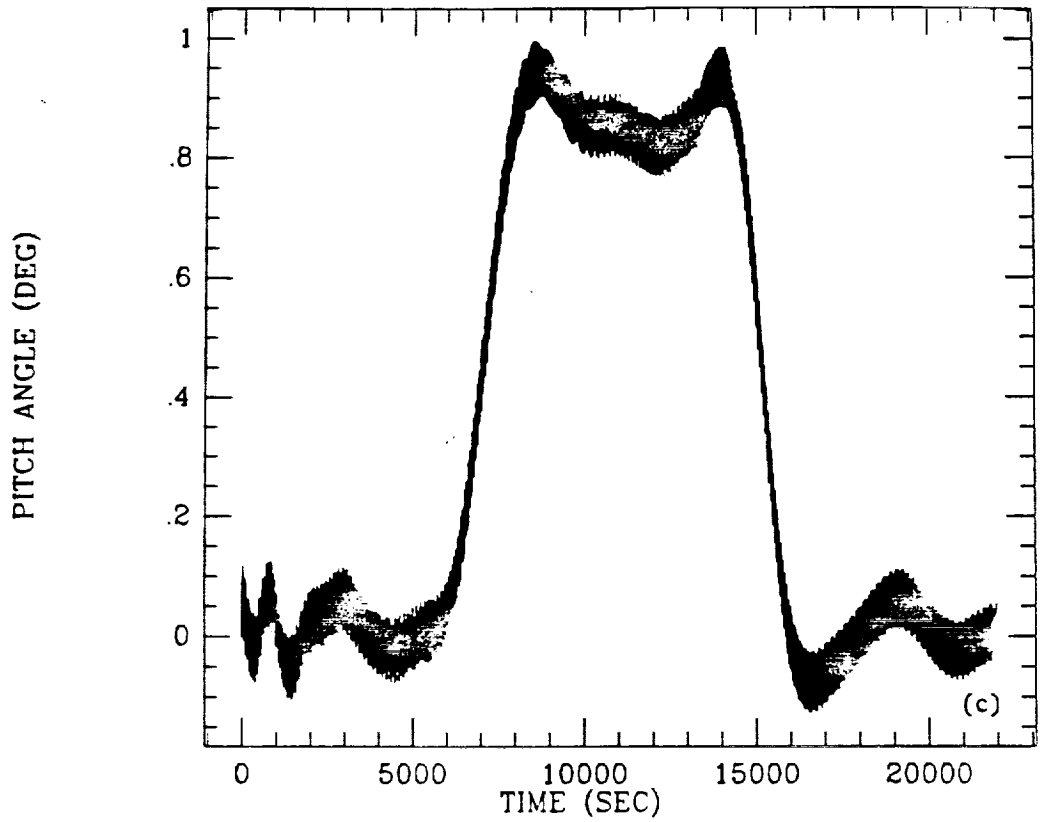

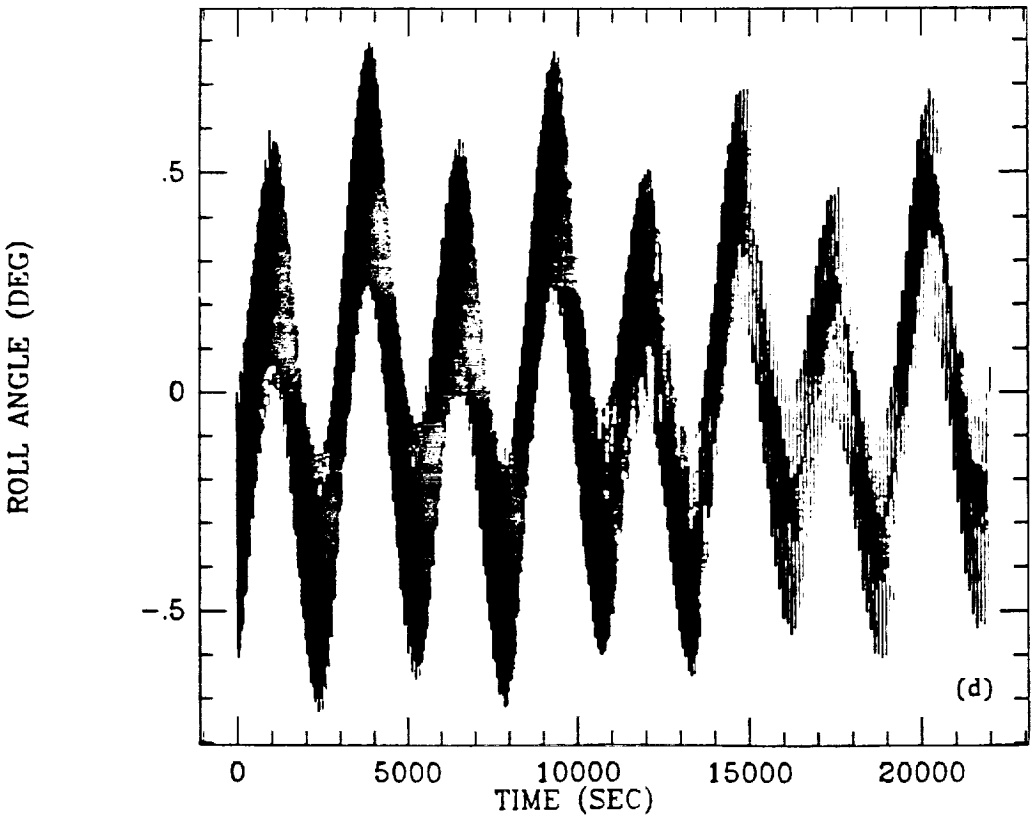

Figures 6(c) and 6(d).

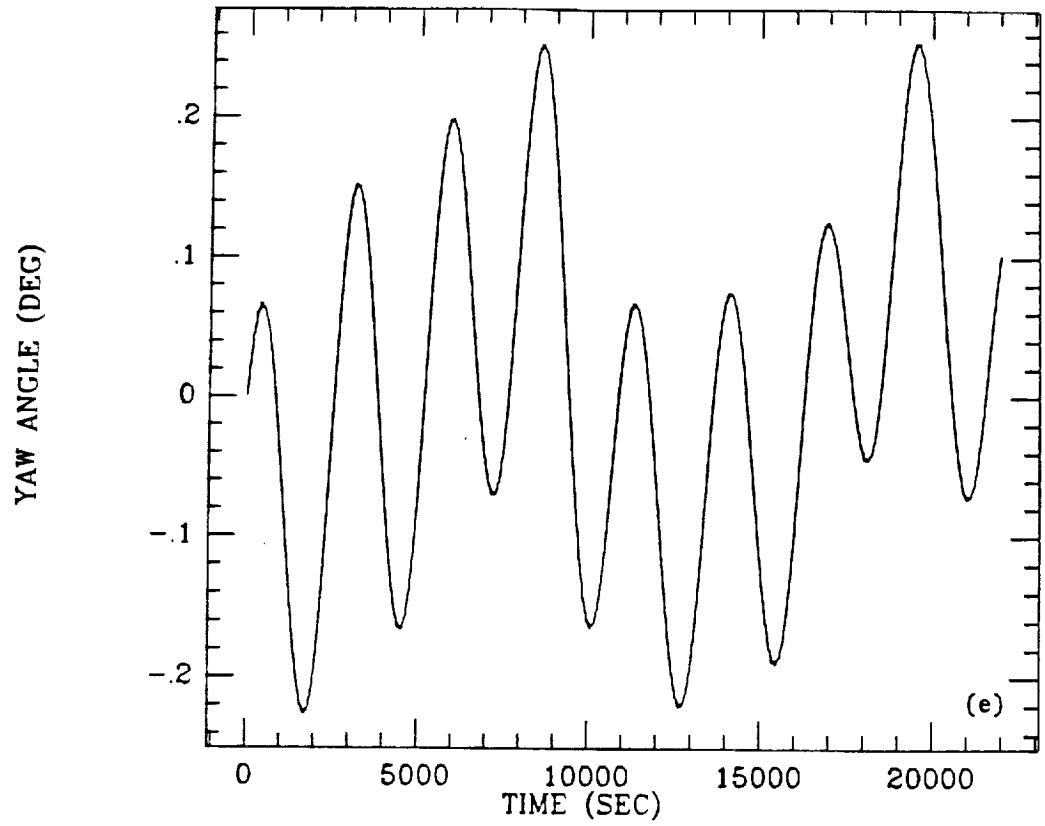

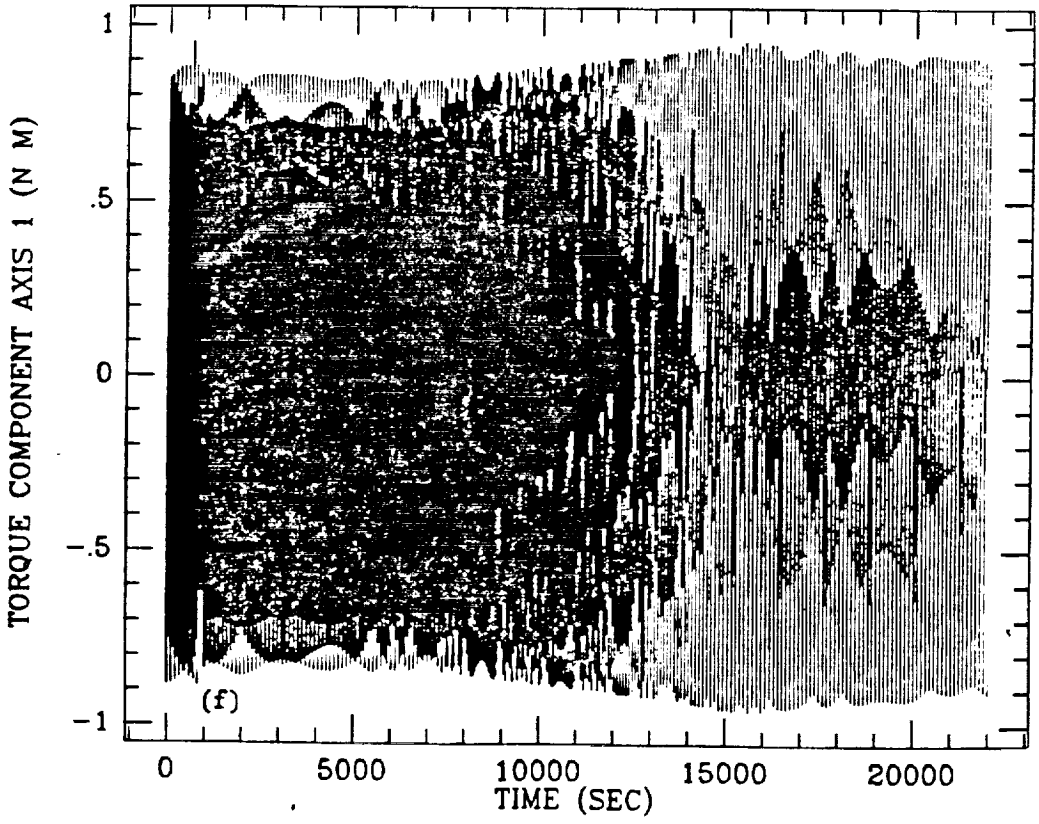

Figures 6(e) and 6(f).

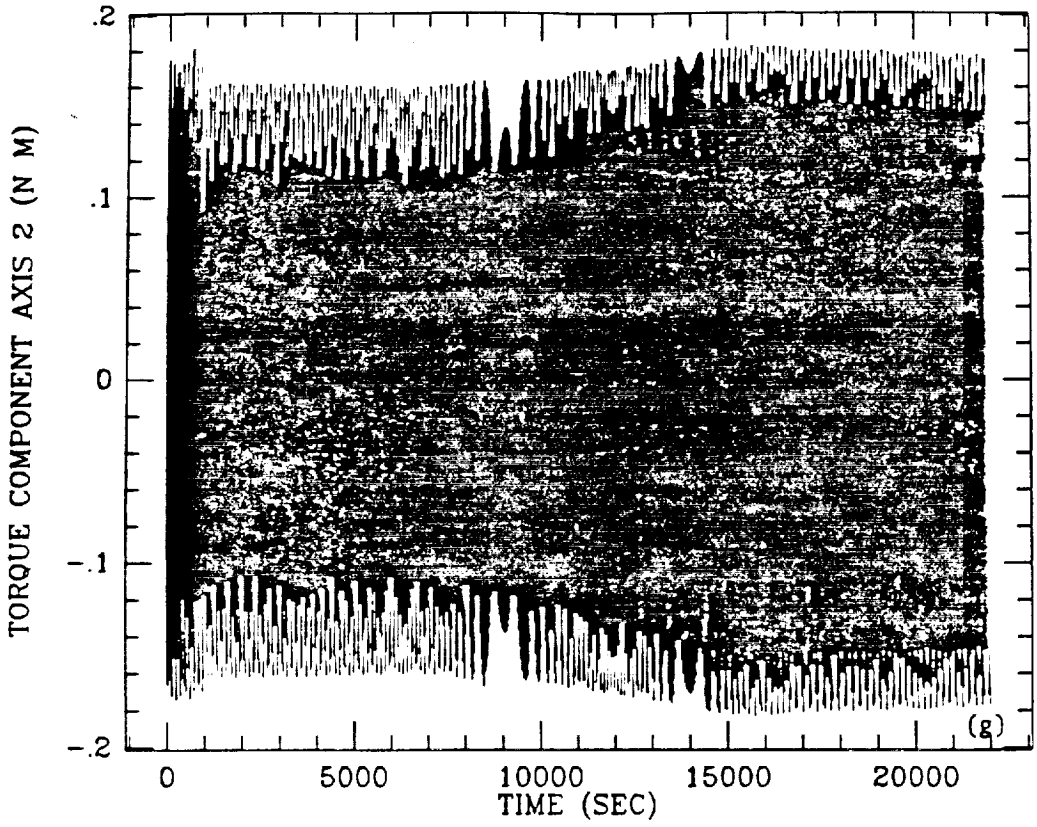

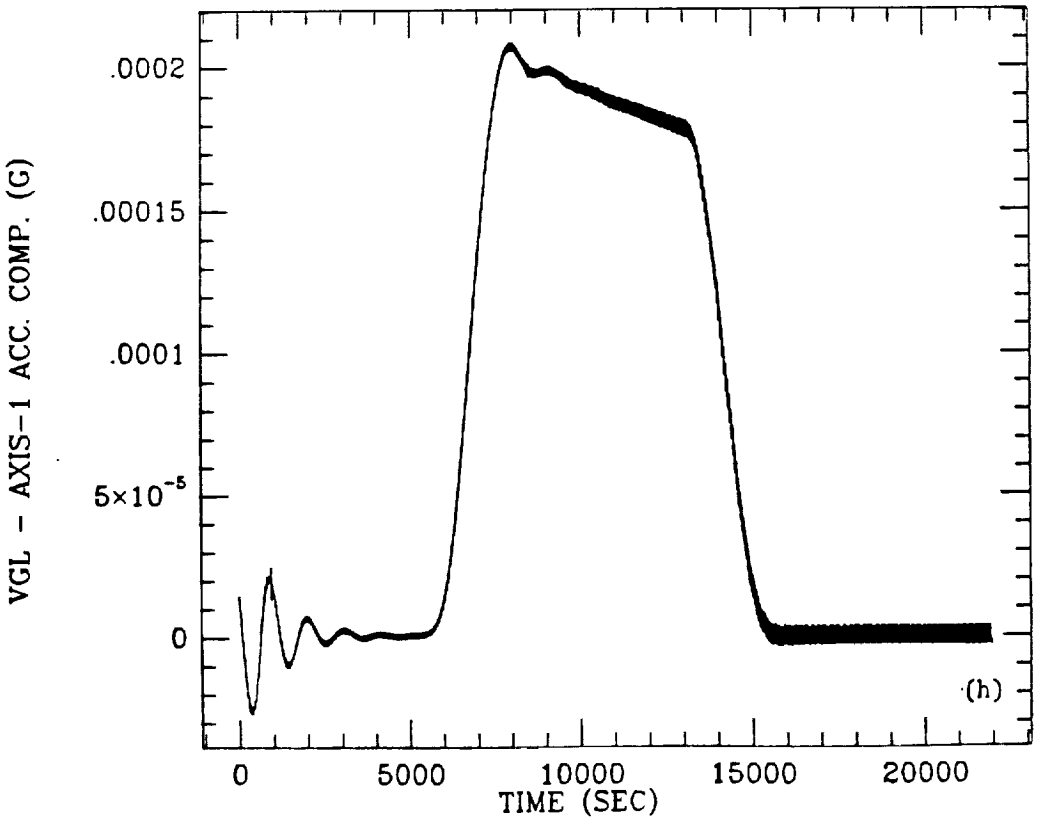

Figures 6(g) and 6(h).

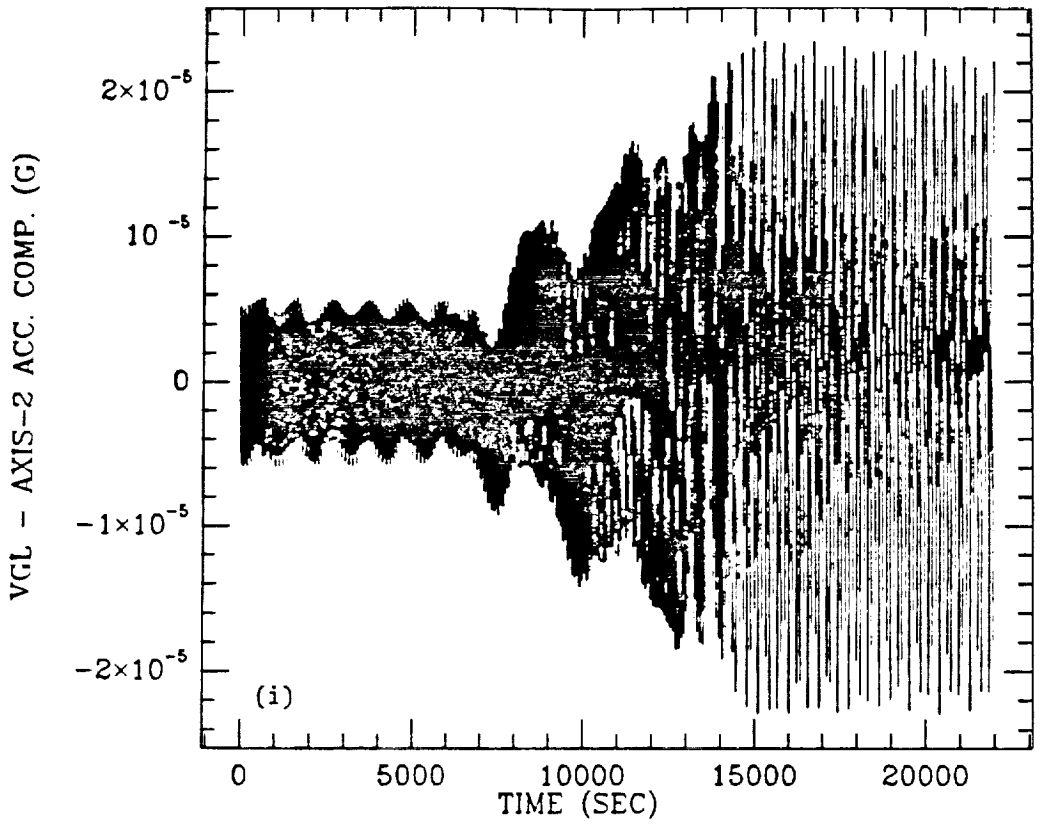

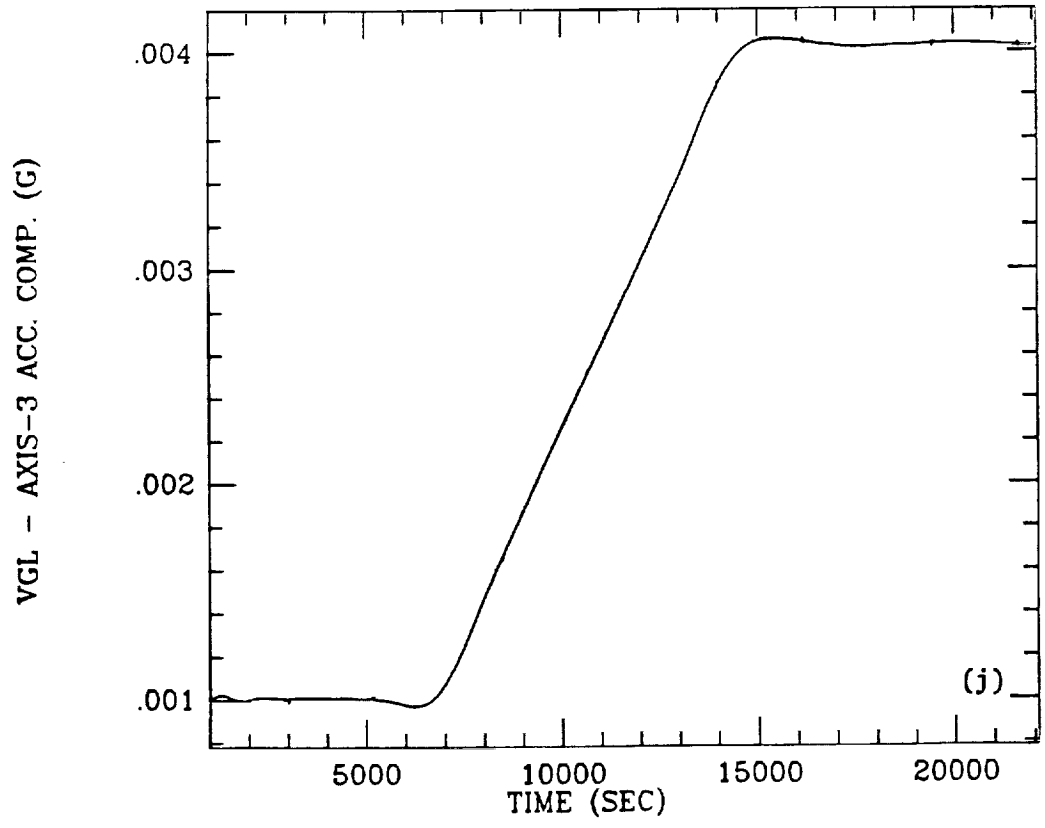

Figures 6(i) and 6(j).